# Theory of bremsstrahlung amplitudes in the soft-photon approximation

M. K. Liou and Z. M. Ding

*Department of Physics and Institute for Nuclear Theory, Brooklyn College of the City University of New York,
Brooklyn, New York 11210*

A general parametrization which enables us to construct all possible approximations to the bremsstrahlung amplitude is applied to explore generalizations of existing soft-photon approximations. We establish the existence of theoretical ambiguity in defining the soft-photon approximations and we show how the bremsstrahlung cross section calculated from a soft-photon amplitude depends on the parameters. We also show that if the bremsstrahlung spectrum exhibits resonant structure, then the position of this structure $K_\gamma$ and its width $\Gamma_\gamma$ can be predicted by either performing the detailed bremsstrahlung calculation or using two simple formulas which relate $K_\gamma$ and $\Gamma_\gamma$ directly to the resonant energy $E_R$ and the width $\Gamma_{el}$ of the resonant structure observed in the elastic scattering cross sections. This new information about $K_\gamma$ and $\Gamma_\gamma$ can be used to study the validity of any bremsstrahlung amplitude. All approximations have been divided into classes, and the following approximations have been systematically studied: (i) the one-energy—one-angle approximation, which is the generalized Low's approximation, and (ii) the two-energy—one-angle approximation, which is the generalized Feshbach-Yennie approximation. We find that all soft-photon amplitudes in the one-energy—one-angle approximation fail to adequately describe the proton-carbon bremsstrahlung ($p^{12}C\gamma$) data near the 1.7-MeV resonance. These amplitudes predict the values of $K_\gamma$ and $\Gamma_\gamma$ which do not agree with the experimental ones. Although the problem comes from both the leading term and the second term of the amplitudes, the major difficulty lies in the derivatives of the elastic scattering amplitudes in the second term. Our study also shows that the limited existing data (which are available only in the soft-photon region, $K < 200$ keV) can be described by many soft-photon amplitudes in the two-energy—one-angle approximation. Since these amplitudes in the two-energy—one-angle approximation predict quite different resonant structure with different values of $K_\gamma$ and $\Gamma_\gamma$ at higher photon energies (200 keV $< K <$ 600 keV), a new $p^{12}C\gamma$ experiment is suggested to test these amplitudes so that the best one can be selected.

## I. INTRODUCTION

During the past three decades, nuclear bremsstrahlung has attracted much attention mainly because of the following reasons: (1) It is the ideal process for investigating the off-shell effects. The use of nucleon-nucleon bremsstrahlung for the study of the off-energy-shell behavior of the two-nucleon interaction is perhaps the most well-known example. In studying nucleon-nucleon bremsstrahlung, one also hopes that from among the many different phenomenological potentials one can distinguish, by its off-energy-shell behavior, the best two-nucleon potential.[1] (2) It can be used to determine the electromagnetic properties of resonances. For instance, the study of pion-proton bremsstrahlung ($\pi^\pm p\gamma$) in the region of the $\Delta(1232)$ resonance was originally suggested for investigating the electromagnetic multipole moments of the $\Delta$ resonance.[2] (3) It can be used to study nuclear reaction. The study of nucleon-nucleus and nucleus-nucleus bremsstrahlung in the vicinity of resonances, for example, was originally motivated by the hope that the measurement of these cross sections could be used as a tool for investigating nuclear reactions.[3–5]

The idea of using bremsstrahlung emission as a tool for investigating nuclear reactions was first proposed by Eisberg, Yennie, and Wilkinson in 1960.[3] Their classical treatment was extended later to a quantum mechanical treatment by Feshbach and Yennie.[4] Briefly, the amplitude which represents the photon emission before nuclear scattering and the amplitude which represents the photon emission after scattering add coherently. Since these two amplitudes differ in phase by $\omega\tau$ ($\omega$ is the radiation frequency, $\tau$ the time delay), the bremsstrahlung cross section evaluated from these two amplitudes (and an internal amplitude obtained through the gauge invariant condition) will contain an interference term which depends upon the time delay $\tau$. For small values of $\omega\tau$, one obtains a typical, smooth bremsstrahlung spectrum with $1/K$ dependence ($K$ is the photon energy). As $\omega\tau$ increases, the interference between the two amplitudes is altered, causing a change in the bremsstrahlung spectrum. For example, when a long-lived resonant state is formed, the bremsstrahlung spectrum will show structure. A quantitative measurement of the bremsstrahlung cross section can then provide a measure of the time delay. This information about the time delay can be used to distinguish unambiguously between a direct nuclear reaction and a compound nuclear reaction. A serious attempt to measure the proton-carbon bremsstrahlung ($p^{12}C\gamma$) cross sections near the 1.7- and 0.5-MeV resonances and to extract useful information about the time delay was made by the Bologna group[6] and the Brooklyn group[7,8] and these results have been confirmed by a group from Tokyo.[9] Each group has clearly observed the resonance struc-

ture in the measured $p^{12}C\gamma$ spectra and used these spectra to extract a delay time of the order of $10^{-20}$ sec. In addition to the $\pi^{\pm}p\gamma$ and $p^{12}C\gamma$ processes, which have already been measured systematically, the proton-oxygen bremsstrahlung ($p^{16}O\gamma$) has also been studied recently by the Brooklyn group.[10]

Most of the bremsstrahlung calculations performed in the past were either model independent calculations or potential model calculations. The model independent calculations are based upon a fundamental theorem, known as the soft-photon theorem or the low-energy theorem for photons. It was first derived by Low[11] and was extended by Adler and Dothan.[12] This theorem states that the first two terms in the series expansion of *the differential bremsstrahlung cross section* (or the bremsstrahlung amplitude) in powers of the photon energy may be calculated exactly in terms of the corresponding elastic amplitude and the electromagnetic constants of the participating particles. Thus, the theorem provides a method for constructing an approximate bremsstrahlung amplitude, which can be used to calculate the bremsstrahlung cross section in terms of the corresponding elastic amplitude.

However, the soft-photon theorem states nothing about the energy and the scattering angle at which the elastic amplitude should be evaluated. Since there are two different energies ($s_i$ and $s_f$) and two different scattering angles ($t_p$ and $t_q$) which can be defined for any bremsstrahlung process, the elastic amplitude can be evaluated at any linear combination of $s_i$ and $s_f$ [$s_{\alpha\beta}=(\alpha s_i+\beta s_f)/(\alpha+\beta)$] and any linear combination of $t_p$ and $t_q$ [$t_{\alpha'\beta'}=(\alpha't_p+\beta't_q)/(\alpha'+\beta')$]. This is the theoretical ambiguity involved in using this theorem, and this ambiguity implies that the prescription used to construct an approximate bremsstrahlung amplitude is by no means unique. This can be seen from the fact that several approximations to the bremsstrahlung amplitude have been proposed by many other authors since Low first put forward his famous soft-photon theorem in 1958.[13] These approximations, called soft-photon approximations (SPA's) or on-shell approximations, have played an important role in the study of bremsstrahlung processes. Among the approximations proposed so far, Low's original SPA, the external emission dominance approximation of Nefkens and Sober (EED),[14] the modified SPA of Nutt, Liu, and Liou,[15] the Feshbach-Yennie approximation (FYA),[16] and many other approximations[17] have been studied and these approximations have been applied to predict either the $\pi^{\pm}p\gamma$ or the $p^{12}C\gamma$ cross sections. But a systematic study of all possible approximations to the amplitude has not yet been done. Such study is required for our work on nuclear bremsstrahlung in the vicinity of a resonance, especially if we wish to find a new approximation which can be used to describe any bremsstrahlung process with or without resonance.

An important connection between the ambiguity problem of the soft-photon theorem and the validity problem of the soft-photon approximations was not fully understood in the past, and the ambiguity problem was completely ignored. Realizing the importance of this problem, we have proposed here a special parametrization which enabled us to generate all possible linear combina-

tions of energies and angles so that the most general bremsstrahlung amplitude can be constructed. We then used this general bremsstrahlung amplitude to study the range of validity of various bremsstrahlung approximations and the nature of the resonant structure predicted by these approximations in the resonance region. To study all approximations systematically, we have divided them into several classes. Two classes have been systematically studied. We have applied the constructed amplitudes to predict the proton-carbon bremsstrahlung cross sections near the 1.7-MeV resonance and the pion-proton bremsstrahlung cross sections near the $\Delta(1232)$ resonance and we have obtained very interesting results. In this article we wish to report the result of our study.

## II. BREMSSTRAHLUNG AMPLITUDE

We consider photon emission accompanying the scattering of two particles $A$ and $B$:

$$A(q_i^{\mu})+B(p_i^{\mu})\rightarrow A(q_f^{\mu})+B(p_f^{\mu})+\gamma(K^{\mu}) .$$

Here, $q_i^{\mu}$ ($q_f^{\mu}$) and $p_i^{\mu}$ ($p_f^{\mu}$) are the initial (final) four-momenta for particles $A$ and $B$, respectively, and $K^{\mu}$ is the four-momentum for the emitted photon. These five momenta are defined in the laboratory frame as

$$q_i^{\mu}=(m+E_i,0,0,q_i) ,$$

$$p_i^{\mu}=(M,0,0,0) ,$$

$$q_f^{\mu}=(m+E_q,q_f\sin\theta_q\cos\phi_q,q_f\sin\theta_q\sin\phi_q,q_f\cos\theta_q) , \quad (1)$$

$$p_f^{\mu}=(M+E_p,p_f\sin\theta_p\cos\phi_p,p_f\sin\theta_p\sin\phi_p,p_f\cos\theta_p) ,$$

$$K^{\mu}=(K,K\sin\theta_\gamma\cos\phi_\gamma,K\sin\theta_\gamma\sin\phi_\gamma,K\cos\theta_\gamma) ,$$

where

$$E_i=(m^2+\mathbf{q}_i^2)^{1/2}-m ,$$

$$E_q=(m^2+\mathbf{q}_f^2)^{1/2}-m ,$$

$$E_p=(M^2+\mathbf{p}_f^2)^{1/2}-M ,$$

and $m$ and $M$ are the masses of particles $A$ and $B$, respectively. These four-momenta satisfy energy-momentum conservation:

$$q_i^{\mu}+p_i^{\mu}=q_f^{\mu}+p_f^{\mu}+K^{\mu} . \quad (2)$$

As we shall see later, the main purpose of this article is to study how a given amplitude (or the bremsstrahlung cross section calculated from a given amplitude) will depend on the choice of the total energy squared and the momentum transfer squared. The answer to this question does not depend on whether the particles ($A$ and $B$) have spin or not. Therefore, for the sake of simplicity, we shall discuss only the spinless case and assume that particles $A$ and $B$ have charges $Z_Ae$ and $Z_Be$, respectively, but they have no spin. In our actual calculations of the $p^{12}C\gamma$ and the $\pi^{\pm}p\gamma$ cross sections, however, the spin of the proton has been taken into consideration.

It is well known that the total bremsstrahlung amplitude $M_{\mu}^{T}$ consists of the external scattering amplitude $M_{\mu}^{E}$ and the internal scattering amplitude $M_{\mu}^{I}$:

$$M_\mu^T = M_\mu^E + M_\mu^I . \tag{3}$$

$M_\mu^E$ can be determined exactly from four external emission diagrams [see Figs. 1(a)—(d)]. In these diagrams, $T_x$ ($x = a,b,c,d$) represent the half-off-shell $T$ matrices which depend upon three Lorentz invariants. Choosing these three invariants to be the total energy squared $s$, the momentum transfer squared $t$, and the square of the invariant mass $\Delta$ of the off-mass-shell leg on which the photon emission occurs, we can define four $T$ matrices as

$$T_a \equiv T(s_a, t_a, \Delta_a) ,$$
$$T_b \equiv T(s_b, t_b, \Delta_b) ,$$
$$T_c \equiv T(s_c, t_c, \Delta_c) , \tag{4}$$
$$T_d \equiv T(s_d, t_d, \Delta_d) ,$$

where

$$s_a = s_c = s_i ,$$
$$s_b = s_d = s_f ,$$
$$t_c = t_d = t_q ,$$
$$t_a = t_b = t_p ,$$
$$\Delta_a = (q_f + K)^2 ,$$
$$\Delta_b = (q_i - K)^2 ,$$
$$\Delta_c = (p_f + K)^2 , \tag{5}$$
$$\Delta_d = (p_i - K)^2 ,$$
$$s_i = (q_i + p_i)^2 = (m + M)^2 + 2ME_i ,$$
$$s_f = (q_f + p_f)^2 = (q_i + p_i - K)^2$$
$$= s_i - 2(q_i + p_i)\cdot K$$
$$= (m + M)^2 + 2M(E_i - K/N) ,$$
$$N = M/[(m + M + E_i) - (E_i^2 + 2mE_i)^{1/2}\cos\theta_\gamma] ,$$
$$t_p = (p_f - p_i)^2 = [q_i - (q_f + K)]^2$$
$$= t_q - 2(q_i - q_f)\cdot K ,$$
$$t_q = (q_f - q_i)^2 = [p_i - (p_f + K)]^2$$
$$= t_p - 2(p_i - p_f)\cdot K .$$

In terms of these four half-off-shell $T$ matrices, $M_\mu^E$ can be written in the form

$$M_\mu^E = Z_A(q_{f\mu}/q_f\cdot K)T_a - Z_A(q_{i\mu}/q_i\cdot K)T_b$$
$$+ Z_B(p_{f\mu}/p_f\cdot K)T_c - Z_B(p_{i\mu}/p_i\cdot K)T_d . \tag{6}$$

$M_\mu^E$ must be expanded in powers of $K$ in order to obtain the leading term of $M_\mu^I$ [the internal emission diagram is shown in Fig. 1(e)] from the gauge invariant condition. Such an expansion is not unique because $T_x$ ($x = a,b,c,d$) can be expanded, in general, about $(s_{\alpha_x\beta_x}(k), t_{\alpha_x'\beta_x'}(k))$, where

$$s_{\alpha_x\beta_x} = (\alpha_x s_i + \beta_x s_f)/(\alpha_x + \beta_x) ,$$
$$t_{\alpha_x'\beta_x'} = (\alpha_x' t_p + \beta_x' t_q)/(\alpha_x' + \beta_x') , \tag{7}$$

and $\alpha_x$, $\beta_x$, $\alpha_x'$, and $\beta_x'$ ($x = a,b,c,d$) are any arbitrary real numbers. Using the following expressions,

$$s_i - s_{\alpha_x\beta_x} = 2[\beta_x/(\alpha_x + \beta_x)](q_i + p_i)\cdot K ,$$
$$s_f - s_{\alpha_x\beta_x} = -2[\alpha_x/(\alpha_x + \beta_x)](q_i + p_i)\cdot K ,$$
$$t_p - t_{\alpha_x'\beta_x'} = -2[\beta_x'/(\alpha_x' + \beta_x')](q_i - q_f)\cdot K , \tag{8}$$
$$t_q - t_{\alpha_x'\beta_x'} = 2[\alpha_x'/(\alpha_x' + \beta_x')](q_i - q_f)\cdot K ,$$

we obtain

$$T_a = T_a^{el} + 2[\beta_a/(\alpha_a + \beta_a)](q_i + p_i)\cdot KT_a^s$$
$$- 2[\beta_a'/(\alpha_a' + \beta_a')](q_i - q_f)\cdot KT_a^t + 2q_f\cdot KT_a^\Delta + \cdots , \tag{9a}$$

$$T_b = T_b^{el} - 2[\alpha_b/(\alpha_b + \beta_b)](q_i + p_i)\cdot KT_b^s$$
$$- 2[\beta_b'/(\alpha_b' + \beta_b')](q_i - q_f)\cdot KT_b^t - 2q_i\cdot KT_b^\Delta + \cdots , \tag{9b}$$
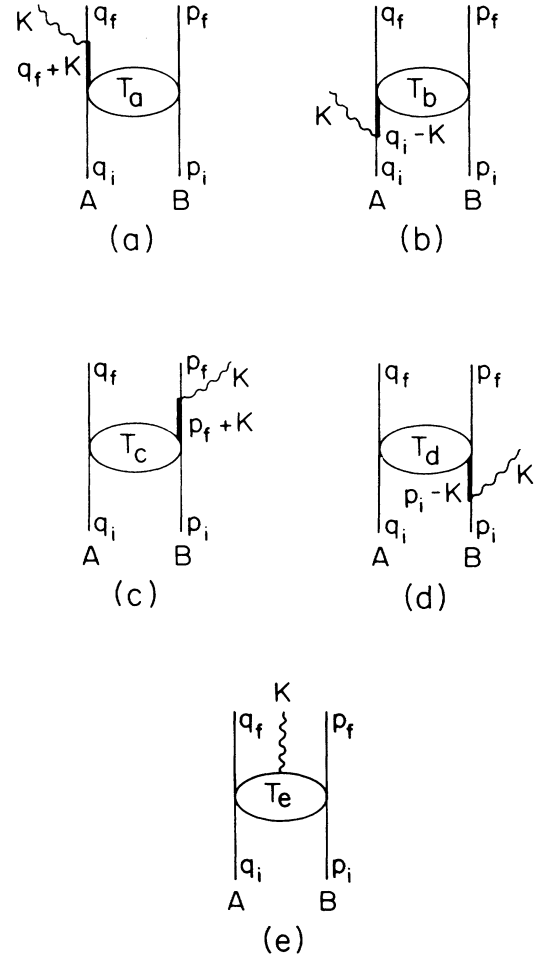






FIG. 1. Feynman diagram for bremsstrahlung: (a)—(d) the external scattering diagrams; (e) the internal scattering diagram.

$$T_c = T_c^{\text{el}} + 2[\beta_c/(\alpha_c + \beta_c)](q_i + p_i) \cdot KT_c^s$$

$$+ 2[\alpha_c'/(\alpha_c' + \beta_c')](q_i - q_f) \cdot KT_c^t + 2p_f \cdot KT_c^\Delta + \cdots ,$$

(9c)

and

$$T_d = T_d^{\text{el}} - 2[\alpha_d/(\alpha_d + \beta_d)](q_i + p_i) \cdot KT_d^s$$

$$+ 2[\alpha_d'/(\alpha_d' + \beta_d')](q_i - q_f) \cdot KT_d^t - 2p_i \cdot KT_d^\Delta + \cdots ,$$

(9d)

$$M_\mu^E = Z_A(q_{f\mu}/q_f \cdot K)T_a^{\text{el}} - Z_A(q_{i\mu}/q_i \cdot K)T_b^{\text{el}} + Z_B(p_{f\mu}/p_f \cdot K)T_c^{\text{el}} - Z_B(p_{i\mu}/p_i \cdot K)T_d^{\text{el}}$$

$$+ (q_i + p_i) \cdot K \{ 2[\beta_a/(\alpha_a + \beta_a)](Z_A q_{f\mu}/q_f \cdot K)T_a^s + 2[\alpha_b/(\alpha_b + \beta_b)](Z_A q_{i\mu}/q_i \cdot K)T_b^s$$

$$+ 2[\beta_c/(\alpha_c + \beta_c)](Z_B p_{f\mu}/p_f \cdot K)T_c^s + 2[\alpha_d/(\alpha_d + \beta_d)](Z_B p_{i\mu}/p_i \cdot K)T_d^s \}$$

$$+ (q_i - q_f) \cdot K \{ -2[\beta_a'/(\alpha_a' + \beta_a')](Z_A q_{f\mu}/q_f \cdot K)T_a^t + 2[\beta_b'/(\alpha_b' + \beta_b')](Z_A q_{i\mu}/q_i \cdot K)T_b^t$$

$$+ 2[\alpha_c'/(\alpha_c' + \beta_c')](Z_B p_{f\mu}/p_f \cdot K)T_c^t - 2[\alpha_d'/(\alpha_d' + \beta_d')](Z_B p_{i\mu}/p_i \cdot K)T_d^t \}$$

$$+ 2(Z_A q_{f\mu}T_a^\Delta + Z_A q_{i\mu}T_b^\Delta + Z_B p_{f\mu}T_c^\Delta + Z_B p_{i\mu}T_d^\Delta) + \cdots ,$$

(9e)

where

$$T_x^s \equiv \partial T_x^{\text{el}}/\partial s_{\alpha_x \beta_x}, \quad T_x^t \equiv \partial T_x^{\text{el}}/\partial t_{\alpha_x' \beta_x'}, \quad T_x^\Delta \equiv \partial T(s_{\alpha_x \beta_x}, t_{\alpha_x' \beta_x'}, \Delta_x)/\partial \Delta_x \quad (x = a, b, c, d) ,$$

(9f)

and $T_x^{\text{el}} \equiv T(s_{\alpha_x \beta_x}, t_{\alpha_x' \beta_x'})$ represents the $T$ matrix evaluated at $s_{\alpha_x \beta_x}$ and $t_{\alpha_x' \beta_x'}$ for the corresponding elastic (nonradiative) process (i.e., the $A$-$B$ elastic scattering process).

To obtain the leading term of $M_\mu^I$, we follow Low's prescription to impose the gauge invariant condition:

$$K^\mu M_\mu^I = -K^\mu M_\mu^E$$

$$= -(Z_A T_a^{\text{el}} - Z_A T_b^{\text{el}} + Z_B T_c^{\text{el}} - Z_B T_d^{\text{el}})$$

$$-2(q_i + p_i) \cdot K \{ Z_A[\beta_a/(\alpha_a + \beta_a)]T_a^s + Z_A[\alpha_b/(\alpha_b + \beta_b)]T_b^s + Z_B[\beta_c/(\alpha_c + \beta_c)]T_c^s + Z_B[\alpha_d/(\alpha_d + \beta_d)]T_d^s \}$$

$$-2(q_i - q_f) \cdot K \{ -Z_A[\beta_a'/(\alpha_a' + \beta_a')]T_a^t + Z_A[\beta_b'/(\alpha_b' + \beta_b')]T_b^t + Z_B[\alpha_c'/(\alpha_c' + \beta_c')]T_c^t - Z_B[\alpha_d'/(\alpha_d' + \beta_d')]T_d^t \}$$

$$-2(Z_A q_f \cdot KT_a^\Delta + Z_A q_i \cdot KT_b^\Delta + Z_B p_f \cdot KT_c^\Delta + Z_B p_i \cdot KT_d^\Delta) + \cdots .$$

(10)

From Eq. (10), we obtain

$$M_\mu^I = -Z_A[(q_{f\mu} + p_{f\mu})/(q_f + p_f) \cdot K]T_a^{\text{el}} + Z_A[(q_{i\mu} + p_{i\mu})/(q_i + p_i) \cdot K]T_b^{\text{el}}$$

$$-Z_B[(q_{f\mu} + p_{f\mu})/(q_f + p_f) \cdot K]T_c^{\text{el}} + Z_B[(q_{i\mu} + p_{i\mu})/(q_i + p_i) \cdot K]T_d^{\text{el}}$$

$$-2(q_i + p_i)_\mu \{ Z_A[\beta_a/(\alpha_a + \beta_a)]T_a^s + Z_A[\alpha_b/(\alpha_b + \beta_b)]T_b^s + Z_B[\beta_c/(\alpha_c + \beta_c)]T_c^s + Z_B[\alpha_d/(\alpha_d + \beta_d)]T_d^s] \}$$

$$-2(q_i - q_f)_\mu \{ -Z_A[\beta_a'/(\alpha_a' + \beta_a')]T_a^t + Z_A[\beta_b'/(\alpha_b' + \beta_b')]T_b^t + Z_B[\alpha_c'/(\alpha_c' + \beta_c')]T_c^t - Z_B[\alpha_d'/(\alpha_d' + \beta_d')]T_d^t \}$$

$$-2(Z_A q_{f\mu}T_a^\Delta + Z_A q_{i\mu}T_b^\Delta + Z_B p_{f\mu}T_c^\Delta + Z_B p_{i\mu}T_d^\Delta) + \cdots .$$

(11)

The total bremsstrahlung amplitude $M_\mu^T$ is then obtained from the sum of $M_\mu^E$ and $M_\mu^I$ [i.e., to combine Eq. (9e) with Eq. (11)], which can be written as

$$M_\mu^T = A_\mu(k)/K + B_\mu(k) + C_\mu(k)K + \cdots ,$$

(12)

where

$$A_\mu(K)/K = +Z_A[q_{f\mu}/q_f \cdot K - (q_{f\mu} + p_{f\mu})/(q_f + p_f) \cdot K]T_a^{\text{el}} - Z_A[q_{i\mu}/q_i \cdot K - (q_{i\mu} + p_{i\mu})/(q_i + p_i) \cdot K]T_b^{\text{el}}$$

$$+ Z_B[p_{f\mu}/p_f \cdot K - (q_{f\mu} + p_{f\mu})/(q_f + p_f) \cdot K]T_c^{\text{el}} - Z_B[p_{i\mu}/p_i \cdot K - (q_{i\mu} + p_{i\mu})/(q_i + p_i) \cdot K]T_d^{\text{el}}$$

(13a)

and

$$B_\mu(K) = +2Z_A[\beta_a/(\alpha_a + \beta_a)][q_{f\mu}/q_f \cdot K - (q_{i\mu} + p_{i\mu})/(q_i + p_i) \cdot K](q_i + p_i) \cdot KT_a^s$$

$$+ 2Z_A[\alpha_b/(\alpha_b + \beta_b)][q_{i\mu}/q_i \cdot K - (q_{i\mu} + p_{i\mu})/(q_i + p_i) \cdot K](q_i + p_i) \cdot KT_b^s$$

$$+ 2Z_B[\beta_c/(\alpha_c + \beta_c)][p_{f\mu}/p_f \cdot K - (q_{i\mu} + p_{i\mu})/(q_i + p_i) \cdot K](q_i + p_i) \cdot KT_c^s$$

$$+ 2Z_B[\alpha_d/(\alpha_d + \beta_d)][p_{i\mu}/p_i \cdot K - (q_{i\mu} + p_{i\mu})/(q_i + p_i) \cdot K](q_i + p_i) \cdot KT_d^s$$

$$- 2Z_A[\beta_a'/(\alpha_a' + \beta_a')][q_{f\mu}/q_f \cdot K - (q_{i\mu} - q_{f\mu})/(q_i - q_f) \cdot K](q_i - q_f) \cdot KT_a^t$$

$$+ 2Z_A[\beta_b'/(\alpha_b' + \beta_b')][q_{i\mu}/q_i \cdot K - (q_{i\mu} - q_{f\mu})/(q_i - q_f) \cdot K](q_i - q_f) \cdot KT_b^t$$

$$+ 2Z_B[\alpha_c'/(\alpha_c' + \beta_c')][p_{f\mu}/p_f \cdot K - (q_{i\mu} - q_{f\mu})/(q_i - q_f) \cdot K](q_i - q_f) \cdot KT_c^t$$

$$- 2Z_B[\alpha_d'/(\alpha_d' + \beta_d')][p_{i\mu}/p_i \cdot K - (q_{i\mu} - q_{f\mu})/(q_i - q_f) \cdot K](q_i - q_f) \cdot KT_d^t .$$

(13b)

We can see from Eqs. (13a) and (13b) that $A_\mu(K)$ depends only on $T_x^{\text{el}}$ $(x=a,b,c,d)$, while $B_\mu(K)$ depends on $T_x^s$ and $T_x^t$. Both $A_\mu(K)$ and $B_\mu(K)$ are independent of the off-shell derivatives $T_x^\Delta$, but they are still functions of $K$. (Since, in general, $\beta_x\neq 0$ and $q_{f\mu}$ and/or $p_{f\mu}$ depend on $K$ implicitly.) As for $C_\mu(K)$ and the coefficients of other higher powers in $K$, they involve the off-shell derivatives which cannot be determined from the corresponding elastic amplitude. Therefore, only the first two terms of the expansion given by Eq. (12) can be used to calculate the bremsstrahlung cross section from a given elastic scattering amplitude. The bremsstrahlung amplitude used in soft-photon approximations can be written in the form

$$M_\mu^{AB} = A_\mu(k)/K + B_\mu(k) . \tag{14}$$

In some calculations, such as the EED approximation of Nefkens and Sober,[14] for example, only the leading term of Eq. (12) has been used. In that case, the amplitude becomes

$$M_\mu^A = A_\mu(k)/K . \tag{15}$$

The amplitude $M_\mu^{AB}$ (or $M_\mu^A$) depends on sixteen parameters, $\alpha_x$, $\beta_x$, $\alpha'_x$, and $\beta'_x$ $(x=a,b,c,d)$, and is therefore very general. By varying these parameters, it can be used to study all possible soft-photon approximations.

## III. SOFT-PHOTON APPROXIMATIONS

To study $M_\mu^{AB}$ and $M_\mu^A$ systematically, we have divided them into the following classes.

(i) One-energy–one-angle approximation (OEOA): This approximation is defined by choosing $\alpha_a=\alpha_b=\alpha_c=\alpha_d=\alpha$, $\beta_a=\beta_b=\beta_c=\beta_d=\beta$, $\alpha'_a=\alpha'_b=\alpha'_c=\alpha'_d=\alpha'$, and $\beta'_a=\beta'_b=\beta'_c=\beta'_d=\beta'$. The amplitude in this approximation which depends only on $s_{\alpha\beta}$ and $t_{\alpha'\beta'}$ can be written as

$$M_\mu^{AB}(s_{\alpha\beta},t_{\alpha'\beta'})=M_\mu^A(s_{\alpha\beta},t_{\alpha'\beta'})+B_\mu(s_{\alpha\beta},t_{\alpha'\beta'}) , \tag{16a}$$

where

$$M_\mu^A(s_{\alpha\beta},t_{\alpha'\beta'})=[Z_A(q_{f\mu}/q_f\cdot K -q_{i\mu}/q_i\cdot K)+Z_B(p_{f\mu}/p_f\cdot K -p_{i\mu}/p_i\cdot K)]T(s_{\alpha\beta},t_{\alpha'\beta'}) , \tag{16b}$$

and

$$B_\mu(s_{\alpha\beta},t_{\alpha'\beta'})=2\{Z_A[\beta/(\alpha+\beta)](q_{f\mu}p_f\cdot K/q_f\cdot K -p_{f\mu})+Z_A[\alpha/(\alpha+\beta)](q_{i\mu}p_i\cdot K/q_i\cdot K -p_{i\mu})$$

$$+Z_B[\beta/(\alpha+\beta)](p_{f\mu}q_f\cdot K/p_f\cdot K -q_{f\mu})+Z_B[\alpha/(\alpha+\beta)](p_{i\mu}q_i\cdot K/p_i\cdot K -q_{i\mu})\}\frac{\partial T(s_{\alpha\beta},t_{\alpha'\beta'})}{\partial s_{\alpha\beta}}$$

$$+2\{Z_A[\beta'/(\alpha'+\beta')](q_{i\mu}/q_i\cdot K -q_{f\mu}/q_f\cdot K)$$

$$-Z_B[\alpha'/(\alpha'+\beta')](p_{i\mu}/p_i\cdot K -p_{f\mu}/p_f\cdot K)\}(q_i -q_f)\cdot K\frac{\partial T(s_{\alpha\beta},t_{\alpha'\beta'})}{\partial t_{\alpha'\beta'}} . \tag{16c}$$

In deriving Eqs. (16b) and (16c), we have used the fact that $K^\mu K_\mu =0$ and we have ignored those terms which are proportional to $K_\mu$ since $\epsilon^\mu K_\mu =0$. Here, $\epsilon^\mu$ is the photon polarization.

The OEOA is a generalization of Low's original SPA. To obtain Low's original result from Eq. (16a), we assume that particle $A$ has charge $e$ and particle $B$ is neutral, i.e., we have $Z_A=1$ and $Z_B=0$. By choosing $\alpha=\beta=1$, $\beta'=0$, and $\alpha'=1$, we obtain, using $\bar{s}=(s_i+s_f)/2$,

$$M_\mu^{AB}(\bar{s},t_p)=(q_{f\mu}/q_f\cdot K -q_{i\mu}/q_i\cdot K)T(\bar{s},t_p)+(q_{f\mu}p_f\cdot K/q_f\cdot K -p_{f\mu}+q_{i\mu}p_i\cdot K/q_i\cdot K -p_{i\mu})\frac{\partial T(\bar{s},t_p)}{\partial \bar{s}} , \tag{17}$$

which is precisely Eq. (1.7) of Ref. 11. Low's original SPA has been extended and applied to calculate cross sections for various bremsstrahlung processes.

The EED approximation used by Nefkens and Sober is also a good example of the OEOA. This approximation uses the amplitude $M_\mu^A$ given by Eq. (16b) and it is evaluated at $(\bar{s},\bar{t})$ or $(s_0,t_0)$. That is, $M_\mu^A(\bar{s},\bar{t})$ or $M_\mu^A(s_0,t_0)$ is used. Here, $\bar{s}=(s_i+s_f)/2$ and $\bar{t}=(t_q+t_p)/2$ are obtained by choosing $\alpha=\beta=\alpha'=\beta'=1$, but $s_0$ and $t_0$, which are defined by

$$s_0=\lim_{k\to 0}s_{\alpha\beta}=s_i$$

and

$$t_0=\lim_{k\to 0}t_{\alpha'\beta'} , \tag{18}$$

are independent of $\alpha$, $\beta$, $\alpha'$, and $\beta'$.

Another interesting example of the OEOA is the modified SPA used by Nutt, Liu, and Liou.[15,18] This approximation uses the amplitude given by Eq. (16a) with the parameters chosen to be $\alpha=1$, $\beta=0$, and

$$\alpha'/\beta' = -(q_f-q_i -\tfrac{1}{2}R_q)\cdot R_q /(p_f-p_i -\tfrac{1}{2}R_p)\cdot R_p ,$$

where $R_q$ and $R_p$ are defined by

$$q_{f\mu}=\lim_{k\to 0}q_{f\mu}+R_{q\mu} ,$$

$$p_{f\mu}=\lim_{k\to 0}p_{f\mu}+R_{p\mu} , \tag{19}$$

$$R_{q\mu}+R_{p\mu}+K_\mu=0 .$$

If Eqs. (19) are used to expand the amplitude further in

powers of $K$, Eqs. (41) and (42) of the Ref. 18 can be obtained. (In Ref. 18, both $A$ and $B$ are assumed to have charge $e$, i.e., $Z_A = Z_B = 1$.) The amplitude obtained in Ref. 18 is evaluated at $(s_0, t_0)$.

(ii) One-energy—two-angle approximation (OETA):

The amplitude in the OETA is evaluated at one energy but two different angles. For example, we can choose $\alpha_a = \alpha_b = \alpha_c = \alpha_d = \alpha$, $\beta_a = \beta_b = \beta_c = \beta_d = \beta$, $\alpha'_a = \alpha'_b = \alpha'_1$, $\alpha'_c = \alpha'_d = \alpha'_2$, $\beta'_a = \beta'_b = \beta'_1$, and $\beta'_c = \beta'_d = \beta'_2$ and obtain the following amplitude:

$$M_\mu^{AB}(s_{\alpha\beta}, t_{\alpha'_1\beta'_1}, t_{\alpha'_2\beta'_2}) = M_\mu^A(s_{\alpha\beta}, t_{\alpha'_1\beta'_1}, t_{\alpha'_2\beta'_2}) + B_\mu(s_{\alpha\beta}, t_{\alpha'_1\beta'_1}, t_{\alpha'_2\beta'_2}) \;, \tag{20a}$$

where

$$M_\mu^A(s_{\alpha\beta}, t_{\alpha'_1\beta'_1}, t_{\alpha'_2\beta'_2}) = +Z_A(q_{f\mu}/q_f \cdot K - q_{i\mu}/q_i \cdot K) T(s_{\alpha\beta}, t_{\alpha'_1\beta'_1}) + Z_B(p_{f\mu}/p_f \cdot K - p_{i\mu}/p_i \cdot K) T(s_{\alpha\beta}, t_{\alpha'_2\beta'_2}) \tag{20b}$$

and

$$\begin{aligned}
B_\mu(s_{\alpha\beta}, t_{\alpha'_1\beta'_1}, t_{\alpha'_2\beta'_2}) = &2Z_A[\beta/(\alpha+\beta)](q_{f\mu}p_f \cdot K/q_f \cdot K - p_{f\mu}) \frac{\partial T(s_{\alpha\beta}, t_{\alpha'_1\beta'_1})}{\partial s_{\alpha\beta}} \\
&+2Z_A[\alpha/(\alpha+\beta)](q_{i\mu}p_i \cdot K/q_i \cdot K - p_{i\mu}) \frac{\partial T(s_{\alpha\beta}, t_{\alpha'_1\beta'_1})}{\partial s_{\alpha\beta}} \\
&+2Z_B[\beta/(\alpha+\beta)](p_{f\mu}q_f \cdot K/p_f \cdot K - q_{f\mu}) \frac{\partial T(s_{\alpha\beta}, t_{\alpha'_2\beta'_2})}{\partial s_{\alpha\beta}} \\
&+2Z_B[\alpha/(\alpha+\beta)](p_{i\mu}q_i \cdot K/p_i \cdot K - q_{i\mu}) \frac{\partial T(s_{\alpha\beta}, t_{\alpha'_2\beta'_2})}{\partial s_{\alpha\beta}} \\
&+2Z_A[\beta'_1/(\alpha'_1+\beta'_1)](q_{i\mu}/q_i \cdot K - q_{f\mu}/q_f \cdot K)(q_i - q_f) \cdot K \frac{\partial T(s_{\alpha\beta}, t_{\alpha'_1\beta'_1})}{\partial t_{\alpha'_1\beta'_1}} \\
&-2Z_B[\alpha'_2/(\alpha'_2+\beta'_2)](p_{i\mu}/p_i \cdot K - p_{f\mu}/p_f \cdot K)(q_i - q_f) \cdot K \frac{\partial T(s_{\alpha\beta}, t_{\alpha'_2\beta'_2})}{\partial t_{\alpha'_2\beta'_2}} \;.
\end{aligned} \tag{20c}$$

An amplitude used by a UCLA group in the calculation of the $\pi^\pm p\gamma$ cross section is a good example of this approximation. That amplitude, which is obtained by choosing $\alpha = \beta = 1$, $\alpha'_1 = \beta'_2 = 1$, and $\alpha'_2 = \beta'_1 = 0$, is evaluated at $(\bar{s}, t_p)$ and $(\bar{s}, t_q)$.

(iii) Two-energy—one-angle approximation (TEOA): The amplitude in the TEOA is evaluated at a common momentum-transfer-squared $t_{\alpha'\beta'}$ (i.e., we choose $\alpha'_a = \alpha'_b = \alpha'_c = \alpha'_d = \alpha'$ and $\beta'_a = \beta'_b = \beta'_c = \beta'_d = \beta'$) and two different energies which can be chosen from $s_{\alpha_x\beta_x}$ $(x = a,b,c,d)$. An important example of this approximation can be obtained by choosing $\alpha_a = \alpha_c = \alpha_1$, $\alpha_b = \alpha_d = \alpha_2$, $\beta_a = \beta_c = \beta_1$, and $\beta_b = \beta_d = \beta_2$ leading to the following amplitude:

$$M_\mu^{AB}(s_{\alpha_1\beta_1}, s_{\alpha_2\beta_2}, t_{\alpha'\beta'}) = M_\mu^A(s_{\alpha_1\beta_1}, s_{\alpha_2\beta_2}, t_{\alpha'\beta'}) + B_\mu(s_{\alpha_1\beta_1}, s_{\alpha_2\beta_2}, t_{\alpha'\beta'}) \;, \tag{21a}$$

where

$$\begin{aligned}
M_\mu^A(s_{\alpha_1\beta_1}, s_{\alpha_2\beta_2}, t_{\alpha'\beta'}) = &[Z_A q_{f\mu}/q_f \cdot K + Z_B p_{f\mu}/p_f \cdot K - (Z_A + Z_B)(q_{f\mu} + p_{f\mu})/(q_f + p_f) \cdot K] T(s_{\alpha_1\beta_1}, t_{\alpha'\beta'}) \\
&- [Z_A q_{i\mu}/q_i \cdot K + Z_B p_{i\mu}/p_i \cdot K - (Z_A + Z_B)(q_{i\mu} + p_{i\mu})/(q_i + p_i) \cdot K] T(s_{\alpha_2\beta_2}, t_{\alpha'\beta'})
\end{aligned} \tag{21b}$$

and

$$\begin{aligned}
B_\mu(s_{\alpha_1\beta_1}, s_{\alpha_2\beta_2}, t_{\alpha'\beta'}) = &2[\beta_1/(\alpha_1+\beta_1)][Z_A q_{f\mu}/q_f \cdot K + Z_B p_{f\mu}/p_f \cdot K - (Z_A + Z_B)(q_{i\mu} + p_{i\mu})/(q_i + p_i) \cdot K] \\
&\times (q_i + p_i) \cdot K \frac{\partial T(s_{\alpha_1\beta_1}, t_{\alpha'\beta'})}{\partial s_{\alpha_1\beta_1}} \\
&+2[\alpha_2/(\alpha_2+\beta_2)][Z_A q_{i\mu}/q_i \cdot K + Z_B p_{i\mu}/p_i \cdot K - (Z_A + Z_B)(q_{i\mu} + p_{i\mu})/(q_i + p_i) \cdot K] \\
&\times (q_i + p_i) \cdot K \frac{\partial T(s_{\alpha_2\beta_2}, t_{\alpha'\beta'})}{\partial s_{\alpha_2\beta_2}} \\
&-2Z_A[\beta'/(\alpha'+\beta')][q_{f\mu}/q_f \cdot K - (q_{i\mu} - q_{f\mu})/(q_i - q_f) \cdot K](q_i - q_f) \cdot K \frac{\partial T(s_{\alpha_1\beta_1}, t_{\alpha'\beta'})}{\partial t_{\alpha'\beta'}} \\
&+2Z_A[\beta'/(\alpha'+\beta')][q_{i\mu}/q_i \cdot K - (q_{i\mu} - q_{f\mu})/(q_i - q_f) \cdot K](q_i - q_f) \cdot K \frac{\partial T(s_{\alpha_2\beta_2}, t_{\alpha'\beta'})}{\partial t_{\alpha'\beta'}} \\
&+2Z_B[\alpha'/(\alpha'+\beta')][p_{f\mu}/p_f \cdot K - (q_{i\mu} - q_{f\mu})/(q_i - q_f) \cdot K](q_i - q_f) \cdot K \frac{\partial T(s_{\alpha_1\beta_1}, t_{\alpha'\beta'})}{\partial t_{\alpha'\beta'}} \\
&-2Z_B[\alpha'/(\alpha'+\beta')][p_{i\mu}/p_i \cdot K - (q_{i\mu} - q_{f\mu})/(q_i - q_f) \cdot K](q_i - q_f) \cdot K \frac{\partial T(s_{\alpha_2\beta_2}, t_{\alpha'\beta'})}{\partial t_{\alpha'\beta'}} \;.
\end{aligned} \tag{21c}$$

The approximation defined by this particular amplitude is a generalization of the original FYA,[4,16] which corresponds to $\alpha_1 = \beta_2 = 1$ and $\beta_1 = \alpha_2 = 0$. If $Z_A = 1$, $Z_B = Z$, and $\alpha'/\beta' = -(q_f - q_i - \frac{1}{2}R_q)\cdot R_q/(p_f - p_i - \frac{1}{2}R_p)\cdot R_p$ are used, then we obtain an amplitude which is very similar to Eq. (15) of Ref. 16. (Equation (15) of Ref. 16 can be precisely reproduced if $q_{f\mu}$ and $p_{f\mu}$ are also expanded in powers of $K$ [using Eqs. (19)] before we impose the gauge invariant condition to obtain the leading term of $M'_\mu$.)

(iv) Two-energy—two-angle approximation (TETA): The amplitude in this approximation is evaluated at two different angles, which can be chosen from $t_{\alpha'_x \beta'_x}$ ($x = a,b,c,d$) and two different energies, which can be chosen from $s_{\alpha_x \beta_x}$ ($x = a,b,c,d$). For example, an amplitude can be obtained by choosing $\alpha_a = \alpha_c = \alpha_1$, $\alpha_b = \alpha_d = \alpha_2$, $\beta_a = \beta_c = \beta_1$, $\beta_b = \beta_d = \beta_2$, $\alpha'_a = \alpha'_b = \alpha'_1$, $\alpha'_c = \alpha'_d = \alpha'_2$, $\beta'_a = \beta'_b = \beta'_1$, and $\beta'_c = \beta'_d = \beta'_2$. We have

$$M_\mu^{AB}(s_{\alpha_1\beta_1}, t_{\alpha'_1\beta'_1}; s_{\alpha_2\beta_2}, t_{\alpha'_2\beta'_2}) = M_\mu^A(s_{\alpha_1\beta_1}, t_{\alpha'_1\beta'_1}; s_{\alpha_2\beta_2}, t_{\alpha'_2\beta'_2}) + B_\mu(s_{\alpha_1\beta_1}, t_{\alpha'_1\beta'_1}; s_{\alpha_2\beta_2}, t_{\alpha'_2\beta'_2}) ,$$ (22a)

where

$$
\begin{aligned}
M_\mu^A(s_{\alpha_1\beta_1}, t_{\alpha'_1\beta'_1}; s_{\alpha_2\beta_2}, t_{\alpha'_2\beta'_2}) = & +Z_A[q_{f\mu}/q_f\cdot K - (q_{f\mu}+p_{f\mu})/(q_f+p_f)\cdot K]T(s_{\alpha_1\beta_1}, t_{\alpha'_1\beta'_1}) \\
& -Z_A[q_{i\mu}/q_i\cdot K - (q_{i\mu}+p_{i\mu})/(q_i+p_i)\cdot K]T(s_{\alpha_2\beta_2}, t_{\alpha'_1\beta'_1}) \\
& +Z_B[p_{f\mu}/p_f\cdot K - (q_{f\mu}+p_{f\mu})/(q_f+p_f)\cdot K]T(s_{\alpha_1\beta_1}, t_{\alpha'_2\beta'_2}) \\
& -Z_B[p_{i\mu}/p_i\cdot K - (q_{i\mu}+p_{i\mu})/(q_i+p_i)\cdot K]T(s_{\alpha_2\beta_2}, t_{\alpha'_2\beta'_2})
\end{aligned}
$$ (22b)

and

$$
\begin{aligned}
B_\mu(s_{\alpha_1\beta_1}, t_{\alpha'_1\beta'_1}; s_{\alpha_2\beta_2}, t_{\alpha'_2\beta'_2}) = & +2Z_A[\beta_1/(\alpha_1+\beta_1)][q_{f\mu}/q_f\cdot K - (q_{i\mu}+p_{i\mu})/(q_i+p_i)\cdot K](q_i+p_i)\cdot K\frac{\partial T(s_{\alpha_1\beta_1}, t_{\alpha'_1\beta'_1})}{\partial s_{\alpha_1\beta_1}} \\
& +2Z_A[\alpha_2/(\alpha_2+\beta_2)][q_{i\mu}/q_i\cdot K - (q_{i\mu}+p_{i\mu})/(q_i+p_i)\cdot K](q_i+p_i)\cdot K\frac{\partial T(s_{\alpha_2\beta_2}, t_{\alpha'_1\beta'_1})}{\partial s_{\alpha_2\beta_2}} \\
& +2Z_B[\beta_1/(\alpha_1+\beta_1)][p_{f\mu}/p_f\cdot K - (q_{i\mu}+p_{i\mu})/(q_i+p_i)\cdot K](q_i+p_i)\cdot K\frac{\partial T(s_{\alpha_1\beta_1}, t_{\alpha'_2\beta'_2})}{\partial s_{\alpha_1\beta_1}} \\
& +2Z_B[\alpha_2/(\alpha_2+\beta_2)][p_{i\mu}/p_i\cdot K - (q_{i\mu}+p_{i\mu})/(q_i+p_i)\cdot K](q_i+p_i)\cdot K\frac{\partial T(s_{\alpha_2\beta_2}, t_{\alpha'_2\beta'_2})}{\partial s_{\alpha_2\beta_2}} \\
& -2Z_A[\beta'_1/(\alpha'_1+\beta'_1)][q_{f\mu}/q_f\cdot K - (q_{i\mu}-q_{f\mu})/(q_i-q_f)\cdot K](q_i-q_f)\cdot K\frac{\partial T(s_{\alpha_1\beta_1}, t_{\alpha'_1\beta'_1})}{\partial t_{\alpha'_1\beta'_1}} \\
& +2Z_A[\beta'_1/(\alpha'_1+\beta'_1)][q_{i\mu}/q_i\cdot K - (q_{i\mu}-q_{f\mu})/(q_i-q_f)\cdot K](q_i-q_f)\cdot K\frac{\partial T(s_{\alpha_2\beta_2}, t_{\alpha'_1\beta'_1})}{\partial t_{\alpha'_1\beta'_1}} \\
& +2Z_B[\alpha'_2/(\alpha'_2+\beta'_2)][p_{f\mu}/p_f\cdot K - (q_{i\mu}-q_{f\mu})/(q_i-q_f)\cdot K](q_i-q_f)\cdot K\frac{\partial T(s_{\alpha_1\beta_1}, t_{\alpha'_2\beta'_2})}{\partial t_{\alpha'_2\beta'_2}} \\
& -2Z_B[\alpha'_2/(\alpha'_2+\beta'_2)][p_{i\mu}/p_i\cdot K - (q_{i\mu}-q_{f\mu})/(q_i-q_f)\cdot K](q_i-q_f)\cdot K\frac{\partial T(s_{\alpha_2\beta_2}, t_{\alpha'_2\beta'_2})}{\partial t_{\alpha'_2\beta'_2}} .
\end{aligned}
$$ (22c)

Various TETA approximations can be obtained from Eq. (22a) by varying parameters $\alpha_1$, $\beta_1$, $\alpha_2$, $\beta_2$, $\alpha'_1$, $\beta'_1$, $\alpha'_2$, and $\beta'_2$. These new approximations have never been studied. Obviously, many more approximations, such as three-energy—one-angle, four-energy—two-angle, etc. can be defined.

## IV. BREMSSTRAHLUNG CROSS SECTION NEAR A RESONANCE

We have used the proton-carbon bremsstrahlung process, $p^{12}C\gamma$, near the 1.7-MeV resonance as an example to study the one-energy—one-angle approximation and the two-energy—one-angle approximation. If $\theta_q$, $\phi_q$, $\theta_\gamma$, $\phi_\gamma$, and $K$ are chosen to be independent, then the bremsstrahlung cross section in the laboratory system can be written as

$$\sigma_\gamma \equiv \frac{d^3\sigma}{d\Omega_q d\Omega_\gamma dK} = \int (2\pi)^{-5}\delta^4(q_i+p_i-q_f-p_f-K)\left[\frac{1}{2}\sum_{\text{pol,spin}}(M_\mu \epsilon^\mu)^+(M^\mu\epsilon_\mu)\right]J(q_f^2 dq_f/2E_q)(d^3p_f/2E_p)(K^2/2K),$$

(23)

where

$$J=e^2 m^2[(p_i\cdot q_i)^2-m^2 M^2]^{1/2}, \quad M_\mu=\bar{u}(q_f,\nu_f)M_\mu^{AB}u(q_i,\nu_i),$$

or

$$M_\mu=\bar{u}(q_f,\nu_f)M_\mu^A u(q_i,\nu_i)$$

and $M_\mu^{AB}$ (or $M_\mu^A$) is given by Eq. (16a) [or Eq. (16b)] for the OEOA approximation and by Eq. (21a) [or Eq. (21b)] for the TEOA approximation (with $Z_A=1$, $Z_B=6$). Here, we should point out that Eqs. (16a) and (21a) were derived originally for two (spin-zero) spinless particles. The main reason why they can also be used for the p$^{12}$C$\gamma$ process, which is a spin-$\frac{1}{2}$—spin-0 case, is because the incident proton energy is about 1.7 MeV and $K \leq 500$ keV (or $K/q_i \ll 1$ and $K/q_f \ll 1$), which allows us to make the following approximations:

$$\bar{u}(q_f,\nu_f)\Gamma_\mu[1/(\slashed{q}_f+\slashed{K}-m)]\simeq\bar{u}(q_f,\nu_f)\gamma_\mu[1/(\slashed{q}_f+\slashed{K}-m)]=\bar{u}(q_f,\nu_f)(q_{f\mu}+\tfrac{1}{2}\gamma_\mu\slashed{K})/q_f\cdot K\simeq\bar{u}(q_f,\nu_f)q_{f\mu}/q_f\cdot K,$$

$$[1/(\slashed{q}_i-\slashed{K}-m)]\Gamma_\mu u(q_i,\nu_i)\simeq[(-q_{i\mu}+\tfrac{1}{2}\slashed{K}\gamma_\mu)/q_i\cdot K]u(q_i,\nu_i)\simeq-q_{i\mu}/q_i\cdot Ku(q_i,\nu_i),$$

where

$$\Gamma_\mu=\gamma_\mu-i\tfrac{1}{2}\lambda\sigma_{\mu\nu}K^\nu/m, \quad \sigma_{\mu\nu}=i[\gamma_\mu,\gamma_\nu]/2,$$

and $\lambda$ Is the proton anomalous magnetic moment. (The contribution from those terms which involve $\lambda$ is negligible in this case.) In this study, particular attention is paid to two energy regions, the energy region very far from any resonance and the energy region of a resonance (in this case the 1.7-MeV resonance), and we shall concentrate mainly on how $M_\mu^{AB}$ and $M_\mu^A$ depend on $s_{\alpha_x\beta_x}$. This can be done by evaluating $T_x^{el}$ at a fixed momentum-transfer-squared $t$ (or at a fixed scattering angle) and varying only $\alpha_x$ and $\beta_x$ (not $\alpha_x'$ and $\beta_x'$).

We have obtained some interesting and important results which can be summarized as follows.

(i) OEOA: In the energy region very far from any resonance, the calculated bremsstrahlung cross section, $\sigma_\gamma^{OEOA}(s_{\alpha\beta},t_{\alpha'\beta'})$, for a given set of $\alpha$, $\beta$, $\alpha'$, and $\beta'$, decreases monotonically with increasing $K$. As $\alpha$ and $\beta$ are varied (keeping $\alpha'$ and $\beta'$ unchanged), we obtain various spectra which form a band. All predictions within this band are equally valid. This theoretical ambiguity cannot be avoided. The ambiguity will be small if the width of this band is very narrow, and in this case any set of $(\alpha,\beta)$ can be used. A set which was most commonly used in the past was $(\alpha,\beta)=(1,1)$. i.e., $s_{\alpha\beta}=\bar{s}=\frac{1}{2}(s_i+s_f)$. On the other hand, if the width of the band is wide, then a set of parameters $(\alpha,\beta,\alpha',\beta')$ which gives the best fit to the data can be determined from the experiment. In the case of p$^{12}$C$\gamma$, the width of the band is found to be very narrow, indicating that the calculated p$^{12}$C$\gamma$ cross sections are quite independent of $\alpha$ and $\beta$. Figure 2 shows a narrow band for $0\leq\beta/\alpha\leq10$ and $t_{\alpha'\beta'}=t_0$. It also shows that the p$^{12}$C$\gamma$ cross sections predicted by the amplitude $M_\mu^{AB}(s_{\alpha\beta},t_0)$ are in good agreement with the experimental data *in the energy region very far away from any resonance.*

In the energy region of a resonance, the bremsstrahlung spectrum calculated from $M_\mu^{AB}(s_{\alpha\beta},t_{\alpha'\beta'})$ or $M_\mu^A(s_{\alpha\beta},t_{\alpha'\beta'})$ will show resonant structure if $s_{\alpha\beta}\neq s_i$ (i.e., if $\beta\neq0$). The predicted structure will be centered about a photon energy $K_\gamma$ in the bremsstrahlung spectrum and it will have a width $\Gamma_\gamma$. Both $K_\gamma$ and $\Gamma_\gamma$ will depend on a factor of the form $(\alpha+\beta)/\beta$ when $\alpha$ and $\beta$ are varied. Furthermore, we have found that $K_\gamma$ and $\Gamma_\gamma$ can be accurately given without actually performing a complicated bremsstrahlung calculation. As shown in Appendix A, if we assume that the cross section $\sigma_{el}$ of the corresponding elastic scattering process exhibits a resonance with the resonance energy $E_R$ and the width $\Gamma_{el}$, then we obtain, based purely on kinematical arguments, the following expressions for
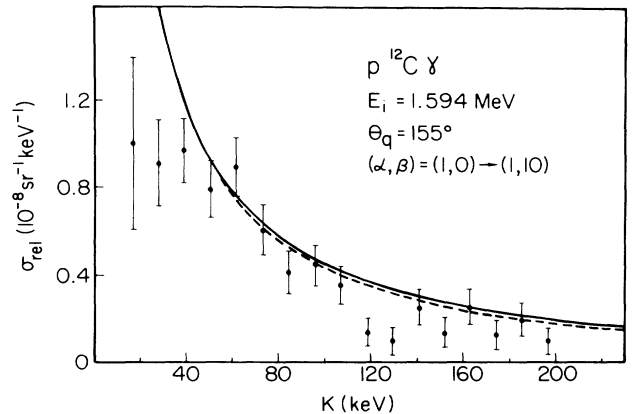


FIG. 2. The relative p$^{12}$C$\gamma$ cross section $\sigma_{rel}$ as a function of photon energy $K$ at an incident proton energy of 1.594 MeV. The solid band represents the calculation using the amplitude $M_\mu^A(s_{\alpha\beta},t_0)$ in the OEOA approximation with $(\alpha,\beta)$ changing from (1,0) to (1,10) and the dashed band represents the calculation using the amplitude $M_\mu^{AB}(s_{\alpha\beta},t_0)$ in the OEOA approximation with $(\alpha,\beta)$ changing from (1,0) to (1,10). The data are from Ref. 7.

$K_\gamma$ and $\Gamma_\gamma$:

$$K_\gamma = K_0(\alpha+\beta)/\beta, \quad \beta \neq 0 \tag{24}$$

$$\Gamma_\gamma = N\Gamma_{\mathrm{el}}(\alpha+\beta)/\beta, \tag{25}$$

where

$$K_0 = (E_i - E_R)N,$$

$$N = M/[(m+M+E_i) - (E_i^2+2mE_i)^{1/2}\cos\theta_\gamma].$$

Equations (24) and (25) enable us to predict (within 10% error) the values of $K_\gamma$ and $\Gamma_\gamma$ in terms of the observed values of $E_R$ and $\Gamma_{\mathrm{el}}$. The dependence of $K_\gamma$ and $\Gamma_\gamma$ on $\alpha$ and $\beta$ is very interesting. It implies that $\alpha$ and $\beta$ can be determined experimentally, by comparing the predicted structure with the observed one, and selecting the best approximation for $\sigma_\gamma^{\mathrm{OEOA}}$ in the resonance region.

In order to compare with the Brooklyn data,[7] we have calculated the p$^{12}$C$\gamma$ cross section relative to the p$^{12}$C elastic cross section, $\sigma_{\mathrm{rel}}^{\mathrm{OEOA}} = \sigma_\gamma^{\mathrm{OEOA}}/\sigma_{\mathrm{el}}$, as a function of $K$ near the 1.7-MeV resonance. Some results of the calculated $\sigma_{\mathrm{rel}}^{\mathrm{OEOA}}$ at $E_i = 1.88$ MeV for $\theta_q = 155°$ are shown in Fig. 3. As we have already mentioned, we have concentrated mainly on how $\sigma_{\mathrm{rel}}^{\mathrm{OEOA}}$ depends on $s_{\alpha\beta}$. Therefore, a fixed momentum-transfer-squared $t_{\alpha'\beta'}$ has been used in all these calculations. We have chosen $t_{\alpha'\beta'}$ to be $\bar{t} = \frac{1}{2}(t_q+t_p)$ or $t_0 = \lim_{k\to 0} t_{\alpha'\beta'}$. The values of $(\alpha,\beta)$ for those spectra labeled I, II, and III in Fig. 3 are (1,0.5), (1,1), and (1,2), respectively, and $t_{\alpha'\beta'}$ used in these calculations is $t_0$. Note that the spectra with label II calculated from the parameters $(\alpha,\beta) = (1,1)$ are identical to the spectra calculated in Low's original approximation. These figures show clearly that every spectrum exhibits resonant structure in the form of a peak. In Fig. 3(a) the spectra are calculated from $M_\mu^A(s_{\alpha\beta},t_0)$. As we know, the levels associated with the 1.7-MeV resonance are two closely spaced levels of $\frac{5}{2}^+$ and $\frac{3}{2}^-$ in the compound nu-

cleus $^{13}$N. Since the main resonant peak in every spectrum arises from the level of $\frac{5}{2}^+$, we can use $E_R = 1.734$ keV to predict the position of the main resonant peak from Eq. (24). Using $N = \frac{12}{13}$, the values of $K_\gamma$ calculated from Eq. (24) are 404, 269.6, and 202 keV for spectra I, II, and III, respectively. These values are to be compared with the following exact values calculated from $\sigma_{\mathrm{rel}}^{\mathrm{OEOA}}$: 405, 270, and 204 keV. The agreement is excellent. We have also found that the values of $\Gamma_\gamma$ calculated from Eq. (25) are in very good agreement with those calculated from $\sigma_{\mathrm{rel}}^{\mathrm{OEOA}}$. In Fig. 3(b) the spectra are calculated from the amplitude $M_\mu^{AB}(s_{\alpha\beta},t_0)$. The giant peaks obtained in these calculations arise mainly from the term involving $\partial T^{\mathrm{el}}/\partial s_{\alpha\beta}$ in $B_\mu(k)$. The values of $K_\gamma$ calculated from Eq. (24) are still in good agreement with those calculated from $\sigma_{\mathrm{rel}}^{\mathrm{OEOA}}$. However, because $\sigma_\gamma^{\mathrm{OEOA}}$ is roughly proportional to $|(s_i-s_{\alpha\beta})\partial T^{\mathrm{el}}/\partial s_{\alpha\beta}|^2$ rather than to $\sigma_{\mathrm{el}}/K$, we have slightly modified Eq. (25) to take into account the variation of $\partial T^{\mathrm{el}}/\partial s_{\alpha\beta}$ in the resonance region.
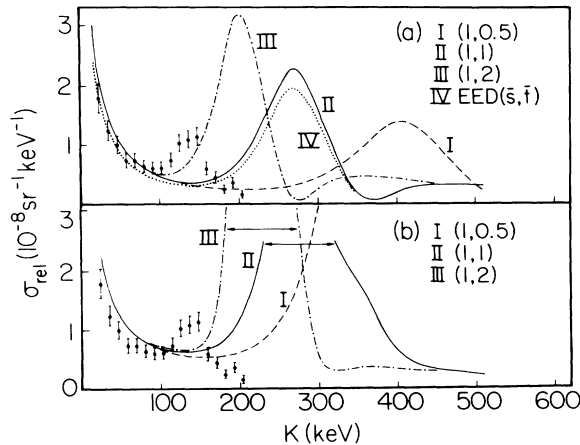
Unfortunately, a comparison with the experimental data shows that the OEOA cannot be used to describe the p$^{12}$C$\gamma$ spectra near the 1.7-MeV resonance. The observed peak appears at $K_0 = (E_i - E_R)N \sim 135$ keV rather than at $K_\gamma = K_0(\alpha+\beta)/\beta$ as predicted by Eq. (24) or $\sigma_{\mathrm{rel}}^{\mathrm{OEOA}}$. If we choose $\beta \gg \alpha$ such that $(\alpha+\beta)/\beta \to 1$, then we can obtain a peak at $K_0$, but the shape of the structure (the giant peak) will be in complete disagreement with the observed one. In order to show this point clearly, we have used $(\alpha,\beta) = (0,1)$ and $t_{\alpha'\beta'} = t_0$ to calculate $\sigma_{\mathrm{rel}}^{\mathrm{OEOA}}$. As shown in Fig. 4, we have obtained a *giant peak* at $K_0 = 135$ keV which is not observed experimentally. We must point out here that this conclusion will remain unchanged even if $t_0$ is replaced by any other $t_{\alpha'\beta'}$ mainly because $t_{\alpha'\beta'}$ (or the corresponding scattering angle) changes slightly with $K$ in the energy region of the calculated spectrum, $0 < K < K' \sim 600$ keV, and $K_{\mathrm{max}} \gg K' > K_\gamma$ in this case. (If $K' < K_\gamma$, then no structure would appear.) Here, $K_{\mathrm{max}}$ is the maximum kinematically allowed photon energy. To demonstrate this point, we have applied the EED approximation, evaluated at $\bar{s} = (s_i+s_f)/2$ and $\bar{t} = (t_q+t_p)/2$, to predict the spectrum in the region $0 < K < 400$ keV. As



FIG. 3. The relative p$^{12}$C$\gamma$ cross section $\sigma_{\mathrm{rel}}$ as a function of photon energy $K$ at an incident proton energy of 1.880 MeV. Curves represent calculations using the amplitude (a) $M_\mu^A(s_{\alpha\beta},t_0)$ in the OEOA approximation and $M_\mu^A(\bar{s},\bar{t})$ in the EED approximation, and (b) $M_\mu^{AB}(s_{\alpha\beta},t_0)$ in the OEOA approximation. The data are from Ref. 7.
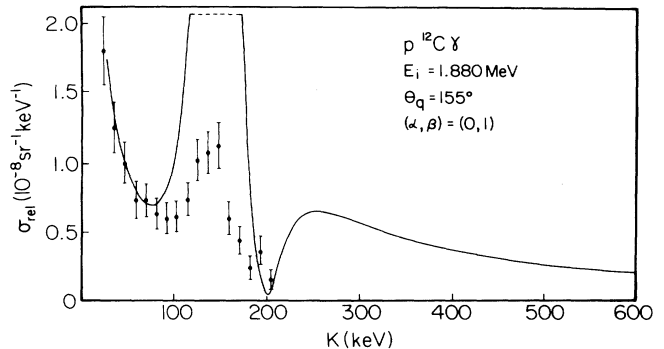


FIG. 4. The relative p$^{12}$C$\gamma$ cross section $\sigma_{\mathrm{rel}}$ as a function of photon energy $K$ at an incident proton energy of 1.880 MeV. The solid curve is calculated from the amplitude $M_\mu^A(s_{\alpha\beta},t_0)$ in the OEOA approximation with $(\alpha,\beta) = (0,1)$ so that $(\alpha+\beta)/\beta = 1$. The data are from Ref. 7.

shown in Fig. 3(a), we have obtained a spectrum with a resonant peak around 270 keV, which is very similar to spectrum II, as expected. Finally, it should also be pointed out that the modified SPA used by Nutt, Liu, and Liou[15,18] does not predict any resonant structure in the energy region of a resonance; it always gives a typical smooth spectrum with $1/K$ dependence. Up to 250 keV, the spectrum predicted by this modified SPA is almost identical to the spectrum labeled I in Fig. 3(a).

Equation (24) can be applied to resolve a mystery found in the pion-proton bremsstrahlung, $\pi^{\pm}p\gamma$, calculation. The $\pi^{\pm}p\gamma$ cross sections near the $\Delta(1232)$ resonance have been calculated by a group from UCLA using an amplitude in the OETA, $M_{\mu}^{AB}(\bar{s},t_p,t_q)$, in order to describe the spectra measured by the group.[2] Instead of getting a resonant peak at the expected photon energy $K_0 = 50$–70 MeV, the calculated cross sections rise steeply with increasing $K$ above 80 MeV.[19] This mysterious result can be explained as follows: Since $s_{\alpha\beta} = \bar{s}$ was used in $M_{\mu}^{AB}$, a resonant peak would be predicted at $K_\gamma = 2K_0$ since $(\alpha+\beta)/\beta = 2$. If $K_0$ is about 60 MeV, then a giant peak will be predicted at 120 MeV (not at 60 MeV, as might be expected). Therefore the predicted spectrum exhibits a minimum around 60 MeV and tends to rise with increasing $K$ above 60 MeV. Our study shows that the giant peak comes from the $B_{\mu}$ term of the amplitude $M_{\mu}^{AB}$, especially the term which involves $\partial T^{el}/\partial \bar{s}$. The predicted spectra will be in better agreement with the data if $M_{\mu}^{A}$ is used. In fact, the EED approximation evaluated at $\bar{s}$ and $\bar{t}$, which is inadequate to describe the p$^{12}$C$\gamma$ data, gives good results for the $\pi^{\pm}p\gamma$ case. As we have discussed in Appendix B, the reasons that the EED predicts monotonically decreasing spectra in this case are that $\bar{t}$ (or the scattering angle) changes substantially with $K$ in the region $0 < K < K' \sim 120$ MeV and that $K_\gamma$ is very close to $K_{max}$ and $K'$, i.e., $K_{max} \sim K' \sim K_\gamma$.

(ii) TEOA: The generalized FYA defined by Eq. (21a) or (21b) is the most important example of the TEOA approximation. The amplitude used in this generalized FYA, which is evaluated at $S_{\alpha_1\beta_1}$ and $S_{\alpha_2\beta_2}$, depends on four parameters $(\alpha_1,\beta_1,\alpha_2,\beta_2)$. In the energy region far from the 1.7-MeV resonance, the calculated $\sigma_{rel}^{TEOA}$ for the p$^{12}$C$\gamma$ process is very similar to the one obtained in the OEOA, because of the smooth energy dependence of the scattering amplitude. In the vicinity of the resonance, however, the generalized FYA predicts a quite different resonant structure from that predicted in the OEOA.

The prediction of the resonant structure is the most interesting and important test of the approximation. By varying four parameters, we obtain various spectra with one or two resonant peaks depending on the values of $S_{\alpha_1\beta_1}$ and $S_{\alpha_2\beta_2}$. If $S_{\alpha_1\beta_1} \neq S_i \neq S_{\alpha_2\beta_2}$ and $S_{\alpha_1\beta_1} \neq S_{\alpha_2\beta_2}$ (i.e., $\beta_1 \neq 0$, $\beta_2 \neq 0$, and $\beta_1 \neq \beta_2$), then two resonant peaks are predicted. Applying Eqs. (24) and (25) to this case, we have $K_\gamma^{(i)} = K_0(\alpha_i+\beta_i)/\beta_i$ and $\Gamma_\gamma^{(i)} = N\Gamma_{el}(\alpha_i+\beta_i)/\beta_i$, $i = 1,2$. On the other hand, if $S_{\alpha_1\beta_1} = S_i$ and $S_{\alpha_2\beta_2} \neq S_i$ (i.e., $\beta_1 = 0$, $\beta_2 \neq 0$), then only one resonant peak is predicted at $K_\gamma^{(2)}$. A typical example is the original FYA, which predicts a single peak at $K_\gamma^{(2)} = K_0$ with $\Gamma_\gamma^{(2)} = N\Gamma_{el}$.

Some results of the calculated $\sigma_{rel}^{TEOA}$ are shown in Figs.

5(a) and 5(b). The values of the parameters $(\alpha_1,\beta_1,\alpha_2,\beta_2)$ for those spectra labeled I, II, III, and IV are (1,0,0,1), (1,1,0,1), (1,0.5, 0,1), and $(1,\frac{1}{3},0,1)$, respectively. Again, $t_0$ is used in these calculations mainly because the calculated cross sections are insensitive to the variation of $t$ in the p$^{12}$C$\gamma$ case. Note that the spectra with label I calculated from the parameters $(\alpha_1,\beta_1,\alpha_2,\beta_2) = (1,0,0,1)$ are identical to the spectra calculated in the original Feshbach-Yennie approximation. Four spectra shown in Fig. 5(a) are calculated from the amplitude $M_{\mu}^{A}(s_{\alpha_1\beta_1},s_{\alpha_2\beta_2},t_0)$. All of these spectra exhibit a common resonant peak (the first peak) at $K_\gamma^{(2)} = K_0 \sim 135$ keV since $(\alpha_2+\beta_2)/\beta_2 = 1$. The spectra II, III, and IV show also a second resonant peak at $K_\gamma^{(1)} = K_0(\alpha_1+\beta_1)/\beta_1$. The existence of the first peak at 135 keV has been verified by the experiment, but no data are available to verify the existence of any other resonant peaks. All four spectra calculated from $M_{\mu}^{A}(s_{\alpha_1\beta_1},s_{\alpha_2\beta_2},t_0)$ are in good agreement with the data in the energy region $K < 100$ keV, but the observed peak cannot be satisfactorily described by any of these calculations.

Four spectra shown in Fig. 5(b) are calculated from the amplitude $M_{\mu}^{AB}(s_{\alpha_1\beta_1},s_{\alpha_2\beta_2},t_0)$. Like those shown in Fig. 5(a), these four spectra have a common peak at 135 keV and every spectrum, except spectrum I, has a second peak at $K_\gamma^{(1)} = K_0(\alpha_1+\beta_1)/\beta_1$. The contribution from the $B_{\mu}(k)$ term of the amplitude $M_{\mu}^{AB}$ is not negligible in the resonance region. It increases the cross section substantially near the second peak (mainly due to the term involving $\partial T_x^{el}/\partial s_{\alpha_1\beta_1}$) and decreases the magnitude of the cross section slightly near the first peak (mainly due to the term involving $\partial T_x^{el}/\partial t_0$). As we can see from this figure, the existing data in the energy region $K < 200$ keV can be
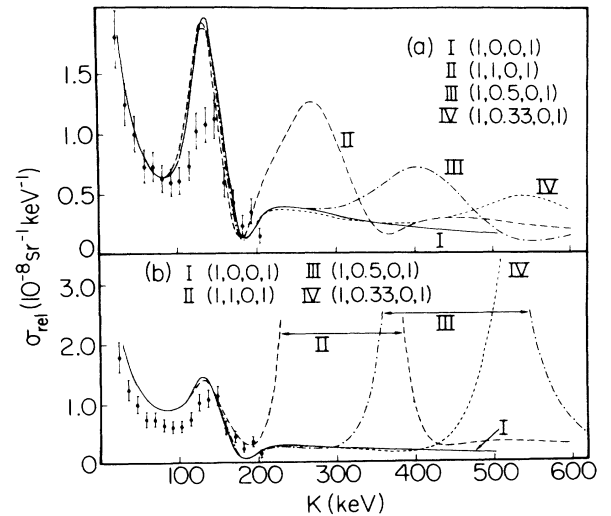


FIG. 5. The relative p$^{12}$C$\gamma$ cross section $\sigma_{rel}$ as a function of photon energy $K$ at an incident proton energy of 1.880 MeV. Curves represent calculations using the amplitude (a) $M_{\mu}^{A}(s_{\alpha_1\beta_1},s_{\alpha_2\beta_2},t_0)$ in the TEOA approximation, and (b) $M_{\mu}^{AB}(s_{\alpha_1\beta_1},s_{\alpha_2\beta_2},t_0)$ in the TEOA approximation. The data are from Ref. 7.

described by all four calculations, but these four calculations give quite different results in the energy region $K > 200$ keV. Thus a precise measurement of the cross sections in the region $K > 200$ keV can be used to determine a set of the best parameters. Finally, it should be pointed out that any calculation with the parameters $(1,\epsilon,0,1)$, where $\epsilon < K_0/(K_{max} - K_0)$, will give a spectrum which is almost identical to spectrum I.

## V. CONCLUSION

We conclude the following.

(i) We have constructed the most general bremsstrahlung amplitude which can be used to study the predictive power of all possible approximations or models, including those well-known approximations that have previously been used. This general amplitude has been divided into many classes of approximations and two classes of approximations have been systematically studied. Special attention is given to the understanding of how these approximations depend on the choice of $s_{\alpha_x\beta_x}$ and $t_{\alpha'_x\beta'_x}$. The main result which we have obtained from our study is that for a given amplitude we know what kind of resonant structure it will give in the resonance region. More precisely, we can predict the position of the structure in photon energy $K_\gamma$ and its width $\Gamma_\gamma$ by either performing a detailed bremsstrahlung calculation or using two simple formulas which relate $K_\gamma$ and $\Gamma_\gamma$ directly to the observed resonant energy $E_R$ and the width $\Gamma_{el}$. This new information can be used to study the validity of any bremsstrahlung amplitude (or to determine which set of $s_{\alpha_x\beta_x}$ and $t_{\alpha'_x\beta'_x}$ is physically acceptable) when the predicted result is compared with the experimental data. The formulas which determine $K_\gamma$ and $\Gamma_\gamma$ in terms of $E_R$ and $\Gamma_{el}$ are very useful. An application of these two formulas is that they can be used to determine the energy region in which both the theoretical prediction and the experimental measurement should be performed.

(ii) We have shown that there is a theoretical ambiguity which cannot be avoided. (This ambiguity cannot be removed by imposing the gauge invariant condition and, to the best of our knowledge, there is no other first principle which can be used to remove this ambiguity.) Mathematically, this ambiguity means that the bremsstrahlung amplitude can be evaluated at $s_{\alpha_x\beta_x}$ and $t_{\alpha'_x\beta'_x}$, where $\alpha_x$, $\beta_x$, $\alpha'_x$, and $\beta'_x$ ($x = a,b,c,d$) are arbitrary real numbers. Since not all of these parameters are physically acceptable and there is no other principle which can be used as a guide to select a set of correct parameters, we rely entirely on experiment to resolve the theoretical ambiguity. That is, we provide all possible results calculated from a given amplitude (or approximation) so that the validity of this amplitude (or approximation) can be determined by comparison with the experimental data.

(iii) We have shown that the one-energy one-angle approximation cannot be used to describe the $p^{12}C\gamma$ data near the 1.7-MeV resonance. This conclusion is drawn from a systematic study of the amplitude in this approximation, which is evaluated at all possible values of $s_{\alpha_x\beta_x}$ and $t_{\alpha'_x\beta'_x}$. Generally speaking, the resonant structure

predicted in the OEOA approximation, including the EED, is quite different from the observed one (different in either the position of the peak or the shape of the structure or both).

(iv) We have shown that the existing experimental $p^{12}C\gamma$ data (available only in the energy region $K < 220$ keV) near the 1.7-MeV resonance can be described by the two-energy—one-angle approximation evaluated at many (infinite) different sets of parameters. We have also shown that different sets of parameters give quite different cross sections in the energy region $220 < K < 600$ keV, but no experimental data are available in that region. Since the data in that region can be used to rule out some sets of parameters which are physically unacceptable, our study provides strong justification for doing new experiments. New experimental data will play a very important role in constructing a new theory.

(v) Although more thorough studies are needed, the results of our investigation seem to indicate that any bremsstrahlung amplitude which involves $\partial T_x^{el}/\partial s_{\alpha_x\beta_x}$ will not be valid in the energy region of a resonance. Since any term involving $\partial T_x^{el}/\partial s_{\alpha_x\beta_x}$ comes from the expansion of $T_x^{el}$ in powers of $s$, which is not valid in the resonance region, and the derivation of every amplitude in the OEOA must involve such expansion, this indication implies that all one-energy approximations would be inadequate, and hence the two-energy approximations would be required to describe the bremsstrahlung cross sections near a resonance. This conclusion agrees with what Kruger and Schultz have found in their study of the validity of the soft-photon approximations when these approximations are applied to calculate the free-free cross sections near a resonance in atomic physics.[20]

## APPENDIX A: THE EXPRESSIONS FOR $K_\gamma$ AND $\Gamma_\gamma$

Let us assume that the elastic scattering cross section, $\sigma_{el}$, of the corresponding elastic scattering process (the $A$-$B$ system) exhibits a resonance with the resonance energy $E_R$ and the width $\Gamma_{el}$, and that the bremsstrahlung spectrum, $\sigma_\gamma^{OEOA}$, calculated from the amplitude $M_\mu^{AB}(s_{\alpha\beta},t_{\alpha'\beta'})$ or $M_\mu^A(s_{\alpha\beta},t_{\alpha'\beta'})$ shows resonant structure, which is centered about a photon energy $K_\gamma$ in the spectrum $\sigma_\gamma^{OEOA}$ and has a width $\Gamma_\gamma$. What we try to derive here are two simple expressions which relate $K_\gamma$ and $\Gamma_\gamma$ directly to $E_R$ and $\Gamma_{el}$, respectively. These expressions are good for the one-energy—one-angle approximation, but they can be extended very easily for the other approximations.

As we know, $M_\mu^{AB}$ (or $M_\mu^A$) involves four different $T$ matrices, $T(s_{\alpha_x\beta_x},t_{\alpha'_x\beta'_x})$, $x = a,b,c,d$. In the OEOA approximation, we have $s_{\alpha_x\beta_x} = s_{\alpha\beta}$ and $t_{\alpha'_x\beta'_x} = t_{\alpha'\beta'}$. Thus all four $T$ matrices are identical and are evaluated at the

same energy $s_{\alpha\beta}$ and the same scattering angle $t_{\alpha'\beta'}$:

$$T(s_{\alpha_x\beta_x}, t_{\alpha'_x\beta'_x}) = T(s_{\alpha\beta}, t_{\alpha'\beta'}) .$$

If we use the following expressions for $s_i$ and $s_f$ [see Eq. (5)],

$$s_i = (m + M)^2 + 2ME_i ,$$

$$s_f = (m + M)^2 + 2M(E_i - K/N) ,$$

we can write $s_{\alpha\beta}$ as a function of $K$ in the form

$$s_{\alpha\beta}(K) = (m + M)^2 + 2M\{E_i - [\beta/(\alpha+\beta)]K/N\} .$$

$$\text{(A1)}$$

Now, suppose the elastic scattering cross section $\sigma_{\mathrm{el}}$ shows a resonance at the resonance energy $E_R$. In terms of $E_R$, we can define $s_R$ as

$$s_R = (m + M)^2 + 2ME_R .$$

$$\text{(A2)}$$

If $\beta \neq 0$ and $s_{\alpha\beta}(0)$ is much greater than $s_R$ (i.e., $E_i \gg E_R$ and far away from any resonance), then a typical bremsstrahlung spectrum with a characteristic $1/K$ dependence will be predicted because the effect of the resonance will be very small. As $K$ increases, $s_{\alpha\beta}(K)$ approaches $s_R$ and the resonance effects become significant. In the energy region of the resonance, i.e., when

$$s_{\alpha\beta}(K_\gamma) = s_R ,$$

$$\text{(A3)}$$

we expect a resonant peak (structure) to appear in the bremsstrahlung spectrum at $K = K_\gamma$. Substituting Eqs. (A1) and (A2) into Eq. (A3) and solving the equation for $K_\gamma$, we obtain

$$K_\gamma = K_0(\alpha+\beta)/\beta, \quad \beta \neq 0$$

$$\text{(A4)}$$

where

$$K_0 = (E_i - E_R)N .$$

$$\text{(A5)}$$

To derive the expression for the width $\Gamma_\gamma$, we write $s_{\alpha\beta}(K)$ in the form

$$s_{\alpha\beta}(K) = (m + M)^2 + 2ME_{\alpha\beta}(K) ,$$

$$\text{(A6)}$$

where

$$E_{\alpha\beta}(K) = E_i - [\beta/(\alpha+\beta)]K/N .$$

$$\text{(A7)}$$

From Eq. (A7), for a given $E_i$ and $\theta_\gamma$, $\Delta E_{\alpha\beta}$ (the change in $E_{\alpha\beta}$) can be written in terms of $\Delta K$ (the change in $K$) as

$$\Delta E_{\alpha\beta} = -[\beta/(\alpha+\beta)]\Delta K/N .$$

$$\text{(A8)}$$

This equation is very useful. For example, if we choose $\Delta E_{\alpha\beta}$ to be the energy difference between the beginning point and the ending point of the resonant structure observed in $\sigma_{\mathrm{el}}$, then $\Delta K$ will be the energy difference between the ending point and the beginning point of the resonant structure predicted in $\sigma_\gamma^{\mathrm{OEOA}}$. Thus, we can define $\Gamma_{\mathrm{el}} = |\Delta E_{\alpha\beta}|$ to be the width of the resonance observed in $\sigma_{\mathrm{el}}$ and $\Gamma_\gamma = |\Delta K|$ to be the width of the resonant structure predicted in $\sigma_\gamma^{\mathrm{OEOA}}$, and write the expression for $\Gamma_\gamma$ in terms of $\Gamma_{\mathrm{el}}$ as

$$\Gamma_\gamma = [(\alpha+\beta)/\beta]N\Gamma_{\mathrm{el}}, \quad \beta \neq 0 .$$

$$\text{(A9)}$$

It should be pointed out that the values of $K_\gamma$ and $\Gamma_\gamma$ obtained from the actual bremsstrahlung calculation [not from Eqs. (A4) and (A9)] may depend on which amplitude, $M_\mu^A$ or $M_\mu^{AB} = M_\mu^A + B_\mu$, is used in the calculation of $\sigma_\gamma^{\mathrm{OEOA}}$. This is because $\sigma_\gamma^{\mathrm{OEOA}}$ can be dominated either by $M_\mu^A$, the leading term of the amplitude, or $B_\mu$, the second term of the amplitude, in the energy region of a resonance. As we have already mentioned, $M_\mu^A$ depends only on $T^{\mathrm{el}} \equiv T(s_{\alpha\beta}, t_{\alpha'\beta'})$, while $B_\mu$ depends on $\partial T^{\mathrm{el}}/\partial s_{\alpha\beta}$ and/or $\partial T^{\mathrm{el}}/\partial t_{\alpha'\beta'}$. Therefore, in the case when the contribution from $B_\mu$ is negligible, $\sigma_\gamma^{\mathrm{OEOA}}$ calculated from either $M_\mu^A$ or $M_\mu^{AB}$ will be about the same and roughly proportional to $\sigma_{\mathrm{el}}/K$ (or $\sigma_{\mathrm{el}}/K$ plus a constant). In this case, the values of $K_\gamma$ and $\Gamma_\gamma$ calculated from Eqs. (A4) and (A9), respectively, will be in very good agreement with those obtained from the exact bremsstrahlung calculation. On the other hand, if $B_\mu \gg M_\mu^A$ in the resonance region, then $\sigma_\gamma^{\mathrm{OEOA}}$ calculated from $M_\mu^{AB}$ will be much greater than that calculated from $M_\mu^A$. Consequently, the width of the resonance $\Gamma_\gamma$ predicted by the amplitude $M_\mu^{AB}$ will be much wider than that predicted by the amplitude $M_\mu^A$ and the position of the resonant peak $K_\gamma$ predicted by these two amplitudes may be different. [$\sigma_\gamma^{\mathrm{OEOA}}$ calculated from $M_\mu^A$ is still roughly proportional to $\sigma_{\mathrm{el}}/K$, but $\sigma_\gamma^{\mathrm{OEOA}}$ calculated from $M_\mu^{AB}$ will be approximately proportional to $|(s_i - s_{\alpha\beta})\partial T^{\mathrm{el}}/\partial s_{\alpha\beta}|^2$. The contribution from the term involving $\partial T^{\mathrm{el}}/\partial s_{\alpha\beta}$ is much more important than that from the term involving $\partial T^{\mathrm{el}}/\partial t_{\alpha'\beta'}$ in the resonance region.] In this case, $K_\gamma$ calculated from Eq. (A4) can be different from that obtained from the actual bremsstrahlung calculation using the amplitude $M_\mu^{AB}$. To get the same value of $K_\gamma$, $E_R$ in Eq. (A4) has to be replaced by $E_R' = E_R - C$, where $C$ is a constant energy, if the expression for $K_\gamma$ given by Eq. (A4) remains unchanged. However, Eq. (A9) for $\Gamma_\gamma$ must be slightly modified to take into account the variation of $\partial T^{\mathrm{el}}/\partial s_{\alpha\beta}$ in the resonance region. Details of the modification will not be discussed here because the result of our study seems to indicate that any amplitude which involves $\partial T^{\mathrm{el}}/\partial s_{\alpha\beta}$ cannot be used to describe the bremsstrahlung spectra in the energy region of a resonance.

### APPENDIX B: THE EED APPROXIMATION

In this appendix we try to explain why the $\pi^\pm p\gamma$ spectrum, $\sigma_{\pi p\gamma}^{\mathrm{EED}}$, calculated in the EED approximation shows a typical bremsstrahlung spectrum with $1/K$ dependence without any resonant structure for most of the photon counters $G_i$ ($i = 1, 2, \ldots, 19$), in good agreement with the experiment.

Nefkens and Sober have calculated $\sigma_{\pi p\gamma}^{\mathrm{EED}}$ from the following formula:

$$\sigma_{\pi p\gamma}^{\mathrm{EED}} = GKD^\mu D_\mu \left[ \frac{d\sigma_{\pi p}(s,t)}{d\Omega} \right] ,$$

$$\text{(B1)}$$

where

$$D^\mu = \mp q_i^\mu/q_i \cdot K - p_i^\mu/p_i \cdot K \pm q_f^\mu/q_f \cdot K + p_f^\mu/p_f \cdot K ,$$

$$G = (e^2/16\pi^3)s^{1/2}q_f^3/\{q_i[q_f^2(s^{1/2} - K) + E_q(q_f \cdot K)]\} ,$$

$$\text{(B2)}$$

and $d\sigma_{\pi p}(s,t)/d\Omega$ is the $\pi^{\pm}p$ elastic scattering cross section evaluated at $s$ and $t$. In the published EED calculations, $d\sigma_{\pi p}/d\Omega$ was evaluated at (i) $s_0$ and $t_0$ and (ii) $\bar{s}$ and $\bar{t}$. Here, $s_0 = s_i = \lim_{k \to 0} s_f$, $t_0 = \lim_{k \to 0} t_p = \lim_{k \to 0} t_q$, $\bar{s} = \frac{1}{2}(s_i + s_f)$, and $\bar{t} = \frac{1}{2}(t_p + t_q)$. The amplitude used in case (i) is identical to our amplitude $M_\mu^A(s_0, t_0)$ given by Eq. (16b) with $Z_B = 1$, $Z_A = \pm 1$ for $\pi^{\pm}$ and the $T$ matrix evaluated at $\lim_{k \to 0} s_{\alpha\beta} = s_0$ and $\lim_{k \to 0} t_{\alpha'\beta'} = t_0$, which can be obtained by choosing $\beta/\alpha = 0$ and

$$\alpha'/\beta' = -(q_f - q_i - \tfrac{1}{2}R_q) \cdot R_q / (p_f - p_i - \tfrac{1}{2}R_p) \cdot R_p .$$

The amplitude used in case (ii) is the same as that used in case (i), except that the $T$ matrix in this case is evaluated at $\bar{s}$ and $\bar{t}$, which can be obtained by choosing $\alpha = \beta = 1$ ($s_{\alpha\beta} = \bar{s}$) and $\alpha' = \beta' = 1$ ($t_{\alpha'\beta'} = \bar{t}$). In order to obtain Eq. (B1), Nefkens and Sober have made another approximation. They have ignored the contribution from the proton anomalous magnetic moment $\lambda$ and they have used the elastic projection operator, $\Lambda(\bar{p}_f) = \lim_{k \to 0}\Lambda(p_f) = \lim_{k \to 0}(\not{p}_f + M)/2M$ in their calculation. This elastic

projection operator, combined together with the amplitude $M_\mu^A$, enable them to write $\sigma_{\pi p\gamma}^{EED}$ in terms of $d\sigma_{\pi p}/d\Omega$ as shown in Eq. (B1).

Now let us explain why $\sigma_{\pi p\gamma}^{EED}$ shows no resonant structure for the $\pi^{\pm}p\gamma$ case and gives a typical bremsstrahlung spectrum with $1/K$ dependence for most of the photon counters $G_i$ ($i = 1, 2, \ldots, 19$), in good agreement with the experiment. In case (i), $d\sigma_{\pi p}/d\Omega$ is evaluated at $s_0$ and $t_0$. Since $s_0$ and $t_0$ are independent of $K$, $d\sigma_{\pi p}/d\Omega$ will not vary with $K$. Therefore, if $\sigma_{\pi p\gamma}^{EED}$ is plotted as a function of $K$, its shape will be determined mainly by the factor $K D^\mu D_\mu$, which is roughly proportional to $1/K$. This is why $\sigma_{\pi p\gamma}^{EED}$ decreases monotonically with increasing $K$. To support this argument, we have calculated $\sigma_{\pi p\gamma}^{EED}$ and we have obtained all spectra which are smooth curves with $1/K$ dependence. Some of these calculations are shown in Figs. 6–8 (the dot-dashed curves). As for case (ii), $d\sigma_{\pi p}/d\Omega$ is evaluated at $\bar{s}$ and $\bar{t}$. Since $\bar{s}$ and $\bar{t}$ are
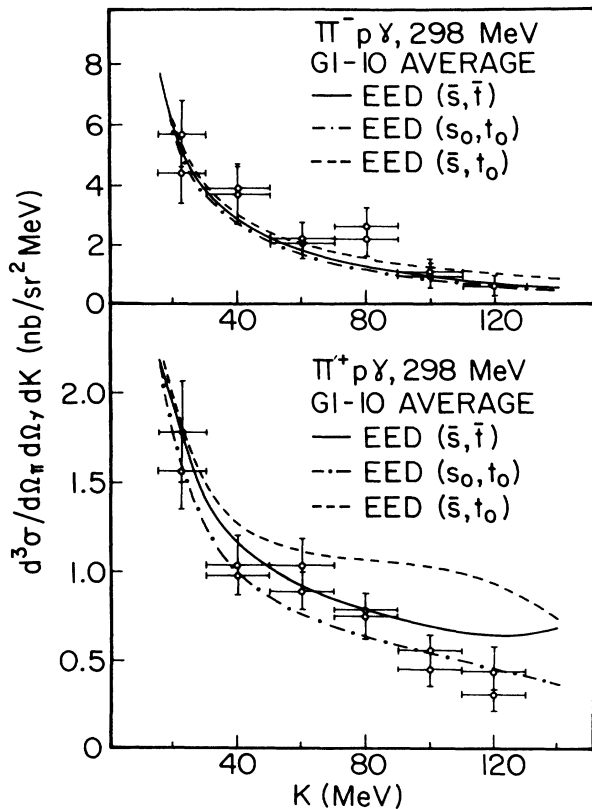


FIG. 6. Comparison of EED predictions (the average cross section over the ten photon counters $G_1$ to $G_{10}$) with the $\pi^{\pm}p\gamma$ data at 298 MeV. The solid curves represent the results of calculation using Eq. (B1) with the elastic $\pi^{\pm}p$ cross section evaluated at $(\bar{s}, \bar{t})$. The dash-dotted curves and the dashed curves are also calculated from Eq. (B1), but with the elastic $\pi^{\pm}p$ cross section evaluated at $(s_0, t_0)$ and $(\bar{s}, t_0)$, respectively. The average experimental data are from Ref. 2.
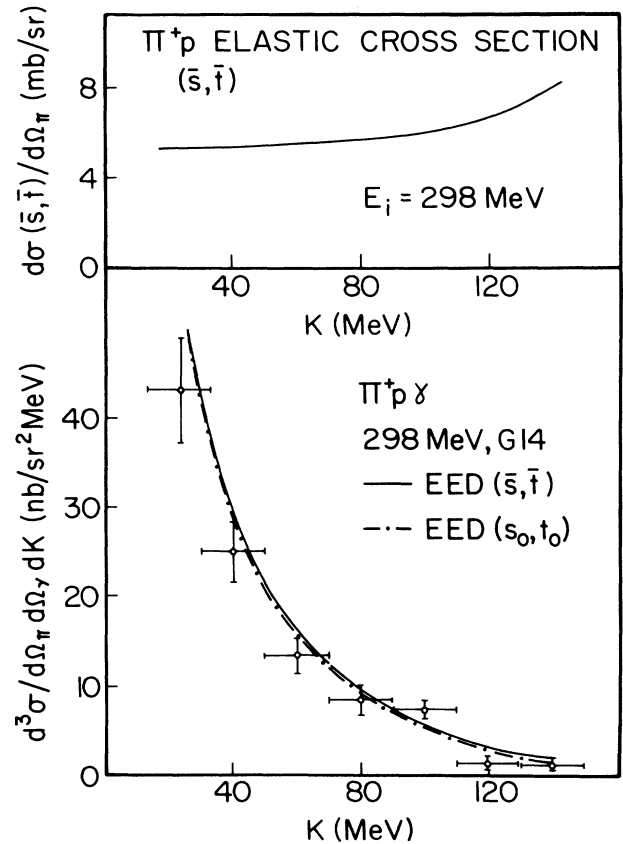


FIG. 7. Top: The $\pi^+p$ elastic cross section, evaluated at $(\bar{s}, \bar{t})$, as a function of photon energy $K$ at an incident pion energy of 298 MeV. Bottom: The $\pi^+p\gamma$ cross section as a function of photon energy $K$ at 298 MeV for the photon counter $G_{14}$. The solid curve represents the result of the EED calculation using Eq. (B1) with the elastic $\pi^+p$ cross section evaluated at $(\bar{s}, \bar{t})$. (This elastic cross section is shown in the top figure.) The dash-dotted curve represents the same calculation, but with the elastic $\pi^+p$ cross section evaluated at $(s_0, t_0)$. The experimental $\pi^+p\gamma$ data are from Ref. 2.
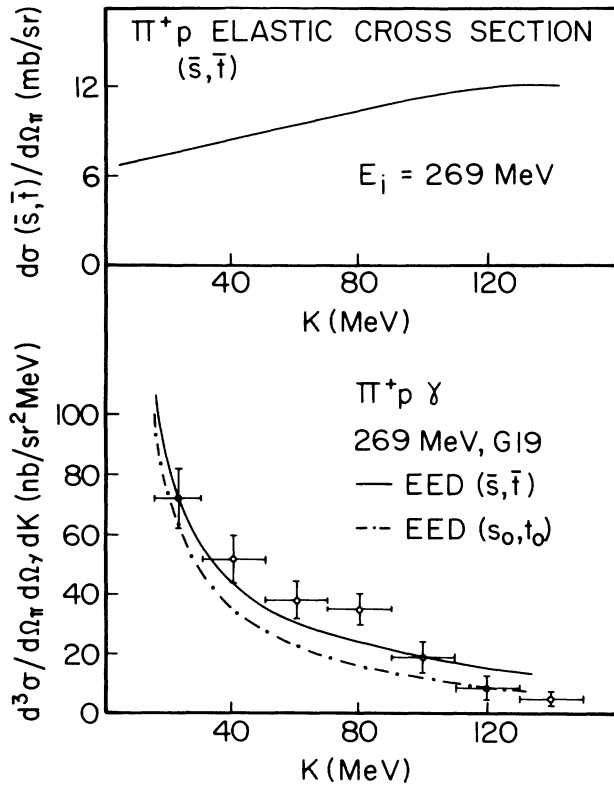
FIG. 8. Same as Fig. 7, but at 269 MeV for $G_{19}$.

counters. Without any resonant structure from the elastic scattering cross section $d\sigma_{\pi p}(\bar{s},\bar{t})/d\Omega$, the shape of $\sigma_{\pi p\gamma}^{EED}$ will be determined mainly by the factor $KD^{\mu}D_{\mu}$. This is the main reason why most of the calculated $\sigma_{\pi p\gamma}^{EED}(\bar{s},\bar{t})$ decrease smoothly with increasing $K$. Some of these calcu-
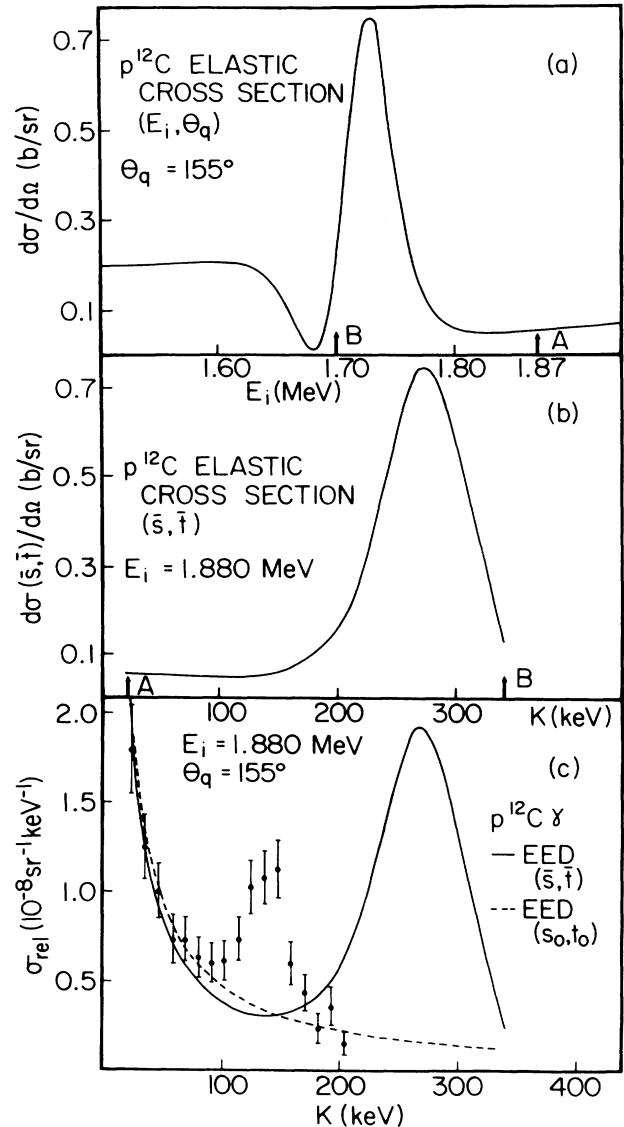


FIG. 9. (a) The $p^{12}C$ elastic cross section as a function of incident proton energy $E_i$ for $\theta_q = 155°$. (b) The $p^{12}C$ elastic scattering cross section, evaluated at $(\bar{s},\bar{t})$, as a function of photon energy $K$ at an incident proton energy of 1.880 MeV. Every point between the arrows $A$ and $B$ on this curve (cross section) corresponds to a point between $A$ and $B$ on the curve shown in (a). Note that the cross section in (a) is plotted as a function of $E_i$ while the cross section in (b) is plotted as a function of $K$ (since $\bar{s}$ is a function of $K$). (c) A comparison of EED predictions with the $p^{12}C\gamma$ data at 1.880 MeV for $\theta_q = 155°$. The solid curve represents the result of the EED calculation using Eq. (B1) with the elastic $p^{12}C$ cross section evaluated at $(\bar{s},\bar{t})$. [This elastic $p^{12}C$ cross section is shown in (b).] The dashed curve represents the same calculation, but with the elastic $p^{12}C$ cross section evaluated at $(s_0,t_0)$. The experimental data are from Ref. 7.

functions of $K$, $d\sigma_{\pi p}/d\Omega$ is no longer independent of $K$. This means that $\sigma_{\pi p\gamma}^{EED}$ will depend on both the factor $KD^{\mu}D_{\mu} \sim 1/K$ and $d\sigma_{\pi p}(\bar{s},\bar{t})/d\Omega$ when $\sigma_{\pi p\gamma}^{EED}$ is plotted as a function of $K$. The fact that $\bar{t}$ depends on $K$ implies that the scattering angle will change with $K$. More precisely, as $K$ increases the scattering angle used in the calculation of $d\sigma_{\pi p}(\bar{s},\bar{t})/d\Omega$ will be shifted from one angle to another. The change in the scattering angle is not small for the $\pi^{\pm}p\gamma$ case at 298 MeV. For $G_{14}$, for example, the scattering angle is changed from 69° at $K=15$ MeV to 100° at 140 MeV. This change will cause $d\sigma_{\pi p}(\bar{s},\bar{t})/d\Omega$ to change slowly and smoothly with increasing $K$. There is another important factor which is directly related to $\bar{s}$. As we know, when $K$ increases, $\bar{s}$ will reach the resonant energy $s_R$ at a photon energy $K_{\gamma}$: $\bar{s}(K_{\gamma})=s_R$. In other words, the predicted resonant peak, if any, is expected to appear at the photon energy $K_{\gamma}$ in the bremsstrahlung spectrum. Our calculation shows that $K_{\gamma}$ is about 110–140 MeV, depending on the photon counters and the incident energy, for the $\pi^{\pm}p\gamma$ case. Since 110–140 MeV is close to the maximum kinematically allowed photon energy $K_{max}$ and the measured photon spectrum is extended to about 120 MeV, no resonant structure can be expected from $d\sigma_{\pi p}(\bar{s},\bar{t})/d\Omega$ for most of the photon counters. [If $K_{\gamma} < K_{max}$ and the photon spectrum is extended to $K'$ with $K_{max} > K' > K_{\gamma}$, then $d\sigma_{\pi p}(\bar{s},\bar{t})/d\Omega$ will show resonant structure in the energy region $0 < K < K'$.] All these factors combined together cause $d\sigma_{\pi p}(\bar{s},\bar{t})/d\Omega$ to vary slowly and smoothly with increasing $K$ (see Figs. 7 and 8) for most of the photon

lations are also shown in Figs. 6—8 (the solid curves). It should be pointed out that if $\bar{t}$ is replaced by $t_0$, which is independent of $K$ (i.e., the scattering angle is fixed), then the calculated cross section $\sigma_{\pi p\gamma}^{\text{EED}}(\bar{s},t_0)$ will show resonant structure, just as we have pointed out in Sec. IV. Some of these calculations are shown in Fig. 6 (the dashed curves).

Although the EED approximation predicts $\pi^{\pm}p\gamma$ cross sections which are in good agreement with the UCLA data, it gives very poor results for the $p^{12}C\gamma$ cross sections (see Sec. IV). There is no contradiction between these two predictions because the predicted cross section depends on the incident bombarding energy, $s_{\alpha\beta}$ and $t_{\alpha'\beta'}$. Different values of $s_{\alpha\beta}$, $t_{\alpha'\beta'}$, and the incident energy would give quite different cross sections in the resonant region. This is exactly the point we try to emphasize in this work. In Fig. 9 the $p^{12}C\gamma$ cross sections $\sigma_{pC\gamma}^{\text{EED}}(s,t)$ are calculated in the EED approximation using Eq. (B1). Here again, $d\sigma_{pC}(s,t)/d\Omega$ is evaluated at (i) $s_0$ and $t_0$ and (ii) $\bar{s}$ and $\bar{t}$. If $d\sigma_{pC}/d\Omega$ is evaluated at $s_0$ and $t_0$, then the predicted $\sigma_{pC\gamma}^{\text{EED}}$ shows no resonant structure as expected for the reason we have already discussed [see the dashed curve in Fig. 9(c)]. If $d\sigma_{pC}/d\Omega$ is evaluated at $\bar{s}$ and $\bar{t}$, on the other hand, then the predicted spectrum shows resonant structure with a peak which appears at $K_\gamma = 2K_0 \sim 270$ keV [since $(\alpha+\beta)/\beta = 2$] [see the solid curve in Fig. 9(c)]. Since the observed peak appears at $K_0 = 135$ keV, the

predicted spectrum is therefore in total disagreement with the experiment. This kind of result is exactly what we have found in our one-energy—one-angle case. To be more precise, the curve for $\sigma_{pC\gamma}^{\text{EED}}$ with $d\sigma_{pC}/d\Omega$ evaluated at $\bar{s}$ and $\bar{t}$ is very similar to the spectrum calculated from the amplitude $M_\mu^A(\bar{s},t_0)$. This is because $\bar{t}$ changes slightly with $K$ in the energy region $10 < K < 400$ keV (the change in the scattering angle is less than $1.0°$), i.e., $\bar{t} \sim t_0$ and $\sigma_{pC\gamma}^{\text{EED}}(\bar{s},\bar{t}) \sim \sigma_{pC\gamma}^{\text{EED}}(\bar{s},t_0)$. We have also found that $K_\gamma \ll K_{\text{max}}$ for this low energy $p^{12}C\gamma$ case. This fact, together with the fact that $\bar{t} \sim t_0$, can be used to explain why the resonant structure is predicted in the $p^{12}C\gamma$ case.

Finally, we should emphasize that the EED approximation of Nefkens and Sober has not only neglected the second term $B_\mu$ of the bremsstrahlung amplitude, but has also ignored the contribution from the proton anomalous magnetic moment $\lambda$. The contribution from these terms is not negligible for the $\pi^{\pm}p\gamma$ processes near the $\Delta(1232)$ resonance. As we have already mentioned in Sec. IV, the contribution from the $B_\mu$ terms causes the calculated $\pi^{\pm}p\gamma$ cross section to rise steeply with increasing $K$ above 80 MeV. And our study shows that the contribution from $\lambda$ does change substantially the magnitude of the $\pi^{\pm}p\gamma$ cross sections for some photon counters. For some cases, the agreement between the predicted cross sections and the UCLA data becomes very poor.

[1]M. I. Sobel and A. H. Cromer, Phys. Rev. **132**, 2698 (1963). An extensive list of references can be obtained from the following review articles: M. L. Halbert, in *Proceedings of Gull Lake Symposium on the Two-body Force in Nuclei*, edited by S. M. Austin and G. M. Crawley (Plenum, New York, 1972); M. J. Moravcsik, Rep. Prog. Phys. **35**, 587 (1972); E. M. Nyman, Phys. Rep. **9**, 179 (1974); M. K. Liou, in *Proceedings of the International Conference on Few-Body Problems in Nuclear and Particle Physics*, Quebec, Canada, edited by R. J. Slobodrian *et al.* (Les Presses de l'Universite Laval, Laval, Quebec, 1975); J. V. Jovanovich, *Nucleon-Nucleon Interactions—1977 (Vancouver)*, AIP Conf. Proc. No. 41, edited by H. Fearing, D. Measday, and S. Strathdee (AIP, New York, 1977).

[2]B. M. K. Nefkens *et al.*, Phys. Rev. D **18**, 3911 (1978), and references therein.

[3]R. M. Eisberg, D. R. Yennie, and D. H. Wilkinson, Nucl. Phys. **18**, 338 (1960).

[4]H. Feshbach and D. R. Yennie, Nucl. Phys. **37**, 150 (1962).

[5]F. Janouch and R. Mach, Nucl. Phys. **A158**, 193 (1970); A. M. Green, in *Proceedings of the International Conference on Few-Body Problems in Nuclear and Particle Physics*, Ref. 1.

[6]C. Maroni, I. Massa, and G. Vannini, Nucl. Phys. **A273**, 429 (1976).

[7]C. C. Trail *et al.*, Phys. Rev. C **21**, 2131 (1980).

[8]P. M. S. Lesser, C. C. Trail, C. C. Perng, and M. K. Liou, Phys. Rev. Lett. **48**, 308 (1982).

[9]H. Taketani, M. Adachi, N. Endo, and T. Suzuki, Phys. Lett. **113B**, 11 (1982); H. Taketani *et al.*, Nucl. Instrum. Methods **196**, 283 (1982).

[10]C. C. Perng, M. K. Liou, Z. M. Ding, P. M. S. Lesser, and C. C. Trail, Phys. Rev. C **29**, 518 (1984); C. C. Perng, Ph.D. thesis, City University of New York.

[11]F. E. Low, Phys. Rev. **110**, 974 (1958).

[12]S. L. Adler and Y. Dothan, Phys. Rev. **151**, 1267 (1966); T. H. Burnett and N. M. Kroll, Phys. Rev. Lett. **20**, 86 (1968).

[13]For a review of these approximations, see L. Heller, in *Proceedings of the International Conference on Few-Body Systems and Nuclear Forces II—Graz, 1978*, Vol. 87 of *Lecture Notes in Physics*, edited by H. Zingl *et al.* (Springer-Verlag, Berlin, 1978), p. 68.

[14]B. M. K. Nefkens and D. I. Sober, Phys. Rev. D **14**, 2434 (1976), and Ref. 2.

[15]M. K. Liou and W. T. Nutt, Phys. Rev. D **16**, 2176 (1977); Nuovo Cimento **46A**, 365 (1978); M. K. Liou and C. K. Liu, Phys. Rev. D **26**, 1635 (1982).

[16]M. K. Liou, C. K. Liu, P. M. S. Lesser, and C. C. Trail, Phys. Rev. C **21**, 518 (1980). See also C. K. Liu, M. K. Liou, C. C. Trail, and P. M. S. Lesser, Phys. Rev. C **26**, 723 (1982).

[17]More references can be found in Refs. 2 and 15.

[18]M. K. Liou, Phys. Rev. D **18**, 3390 (1978).

[19]We must point out here that although the amplitude used by the UCLA group is not valid in the energy region of the $\Delta$ resonance, it will be a good amplitude in the energy region far from the $\Delta$ resonance. The work of Smith *et al.* [D. E. A. Smith *et al.*, Phys. Rev. D **21**, 1715 (1980)] provides further evidence in support of this argument.

[20]H. Kruger and M. Schultz, J. Phys. B **9**, 1899 (1976). The effects of electron-atom scattering resonances on the laser-induced free-free electronic transitions are investigated in this paper. Kruger and Schultz have derived the amplitude (the dipole matrix element) for the free-free transition in a nonrelativistic potential model. Neglecting the contribution from the second-order amplitude (rescattering term), these authors have studied numerically two versions of soft-photon approximations. The first approximation [Eq. (4) of their paper]

M. K. LIOU AND Z. M. DING

inolves a soft-photon amplitude which depends on $T(E_i)$ and $T(E_f)$, i.e., on two energies, $E_i$ and $E_f$. This amplitude can be classified as the two-energy approximation and is similar to the principal (leading) term of the Feshbach-Yennie approximation used in bremsstrahlung calculation. If $T(E_i)$ and $T(E_f)$ in this two-energy amplitude are expanded about a common energy $E$, and if those terms involving the derivatives of $T(E)$ with respect to $E$ [i.e., $\partial T(E)/\partial E, \ldots$] are neglected, one then obtains the second amplitude [Eq. (5) of their paper] which depends on $T(E)$, i.e., only on single energy $E$. This second soft-photon amplitude belongs to the one-energy approximation and is similar to the leading term of Low's approximation used in the bremsstrahlung calculation.

These two soft-photon amplitudes are tested numerically by the authors and they have found that the two-energy approximation gives much better results than the one-energy approximation. Although it has not been discussed explicitly by these authors, the main reason why the one-energy approximation fails to adequately describe the free-free cross sections near a resonance can be understood as follows: The derivation of the one-energy approximation requires the expansions of $T(E_i)$ and $T(E_f)$ in powers of $E$ and such expansions are not valid in the resonance region (the contribution from $\partial T/\partial E$ will be very large). On the other hand, the two-energy approximation which avoids such invalid expansions is expected to be a better approximation.